

Wilfrid Laurier University

Scholars Commons @ Laurier

---

Theses and Dissertations (Comprehensive)

---

2020

## An Evaluation of Ground-Freezing Methods in the Zone of Discontinuous Permafrost, Northwest Territories

Elzbieta Mastej Ms

Wilfrid Laurier University, mast7630@mylaurier.ca

Follow this and additional works at: <https://scholars.wlu.ca/etd>



Part of the [Environmental Engineering Commons](#), [Environmental Monitoring Commons](#), and the [Hydrology Commons](#)

---

### Recommended Citation

Mastej, Elzbieta Ms, "An Evaluation of Ground-Freezing Methods in the Zone of Discontinuous Permafrost, Northwest Territories" (2020). *Theses and Dissertations (Comprehensive)*. 2277.  
<https://scholars.wlu.ca/etd/2277>

This Thesis is brought to you for free and open access by Scholars Commons @ Laurier. It has been accepted for inclusion in Theses and Dissertations (Comprehensive) by an authorized administrator of Scholars Commons @ Laurier. For more information, please contact [scholarscommons@wlu.ca](mailto:scholarscommons@wlu.ca).

**An Evaluation of Ground-Freezing Methods in the Zone of  
Discontinuous Permafrost, Northwest Territories**

by

**Elzbieta Mastej**

**Master of Science in Geography**

**Wilfrid Laurier University, 2020**

**A Thesis submitted to the Faculty of Graduate Studies in partial  
fulfillment of the requirements for the degree of Master of Science  
in Geography**

**Wilfrid Laurier University**

**© Elzbieta Mastej 2020**

## **ABSTRACT**

### **An Evaluation of Ground-Freezing Methods in the Zone of Discontinuous Permafrost, Northwest Territories**

**Elzbieta Mastej**

**Supervisor: Dr William Quinton**

**Wilfried Laurier University**

**Committee Members: Michael Braverman**

**Dr Michael English**

The Canadian subarctic has been one of the most rapidly warming regions on Earth in the last few decades. Permafrost loss is the most conspicuous manifestation of climate change and it is implicated in rapid landscape transition. Permafrost degradation is further exacerbated by anthropogenic disturbances related to resource exploration. Mechanical ground cooling approaches have been investigated in mineral-based substrates with many successful outcomes, however, in peat-based environments they remain largely unexplored. Ground cooling systems are used in application-oriented projects largely pertaining to civil engineering operations. As such, their use in the remote peatland environments range from minimal to non-existent. However, fast rates of climate change and concomitant landscape evolution coupled with increasing socio-economic activity in the North affirm the growing need for the advancement of ground-supporting technologies in peat-based substrates. This study examines the evolution of seven ground cooling systems at Scotty Creek Research Station, NT. The findings of this study will aid in advancing the adaptation of cooling technologies to highly saturated and remote environments.

## **AKNOWLEDGEMENTS**

I would like to acknowledge that Scotty Creek Research Station is located on Treaty 11 land and I would like to thank Dehcho First Nations and Liidlii Kue First Nations for their support and partnership.

I would like to express my deep gratitude to my supervisor Dr William Quinton not only for all of his academic support, guidance and encouragement throughout this research project but also for his outstanding commitment to community partnership and outreach, which augmented my aspiration to explore environmental phenomena in close partnership with the communities. Thank you for giving me the opportunity to embark on this life-changing project!

I would also like to thank my committee members, Michael Braverman for all his expertise, unwavering support and endless patience and Dr Michael English for his expert insight and guidance.

I would like to extend my sincere thanks to the members of Dr Quinton`s Research Group and Faculty and Staff of the Department of Geography and Environmental Studies at Wilfrid Laurier University for their assistance throughout this research.

I also take this opportunity to express a deep sense of gratitude to Dr Jon Warland from University of Guelph for his unparalleled insight into the integral fabric of science and humanity.

# Table of Contents

<b>AKNOWLEDGEMENTS .....</b>	<b>iii</b>
<b>Chapter 1: Introduction .....</b>	<b>1</b>
<b>Chapter 2: An evaluation of ground-freezing methods at Scotty Creek Research Station in the zone of discontinuous permafrost, Northwest Territories .....</b>	<b>9</b>
<b>Abstract .....</b>	<b>9</b>
<b>1. Introduction .....</b>	<b>10</b>
<b>2. Study Site .....</b>	<b>14</b>
<b>3. Methods .....</b>	<b>18</b>
3.1 Thermosyphons-Design Evolution.....	18
3.2 Snow Exclusion Experiment .....	22
3.3 Assessment of the Simple 1-D Heat Conduction Model and Freezing Front Development Analysis .....	24
<b>4. Results and Discussion.....</b>	<b>24</b>
4.1 Thermosyphons .....	24
4.1.1 Two-phase, passive7.....	24
4.1.2 Single-phase, active1 .....	25
4.1.3 Single-phase, active4.....	25
4.1.4 Single-phase, active with a cone .....	26
4.1.5 Insulated and non-insulated coaxial .....	29
4.2 Snow-shading cones.....	30
4.2.1 Inter-site evaluation (between the groups) .....	30
4.2.2 Intra-site evaluation (within each group) .....	31
4.2.3 Evaluation of 1-D heat conduction model for calculating depth of freeze at Cone1 and Cone2.....	33
4.2.4 Ground insulation under Cone5 and under direct snowpack.....	33
4.2.5 Preliminary snow insulation assessment .....	34
4.3 Recommendations .....	35
<b>5. Conclusions.....</b>	<b>37</b>
<b>6. Appendix A-Figures.....</b>	<b>39</b>
<b>Chapter 3: Conclusion.....</b>	<b>55</b>
<b>Chapter 4: References .....</b>	<b>59</b>

## Chapter 1: Introduction

The circumpolar region in the Northern Hemisphere is the most rapidly warming region on Earth in recent decades (Richter-Menge et al., 2017), triggering widespread and irreversible landscape and hydrological changes. Climate change has extensive social impacts, resulting in increased challenges to northern communities and emphasizing the urgent need for mitigation and adaptation strategies. Climate warming in the northern environments is manifested by the changing dynamics of ground thermal regimes and consequent permafrost degradation (Burgess, 2000). The most striking consequence of this changing dynamic is rapid permafrost thaw-induced landcover change, resulting from changes in both geomorphology (Olefeldt et al, 2016) and ecology (Baltzer et al, 2014).

Permafrost underlies approximately 25% of the world's land surface exerting a critical control on water distribution within the northern terrestrial ecosystems (Quinton, 1999) and it is directly linked to landcover configuration (Quinton et al., 2003). Over the last 100-150 years 30%-65% of permafrost on the southern margin of discontinuous zone in north-western Canada has degraded; in some areas the southern boundary migrated northward as far as 120 km between 1964 and 1990 (Simon and Payette, 2009).

The most apparent permafrost-thaw induced transition of forest into wetland (Quinton et al 2011) is governed by regional climatic change as well as localized geophysical and geocryological conditions. However, recent studies identified a positive correlation between increased air temperatures and forest gain along a north-south transect spanning the sporadic-discontinuous permafrost zone (Carpino et al., 2018), which has been proposed to result from increased drainage density (Chasmer and Hopkinson 2017) and evapotranspiration (Warren et al

2018), leading to increased tree productivity (Baltzer et al 2014). These findings emphasize the need for long-term studies to better understand feedback processes over long timescales.

Permafrost is highly implicated in the feedbacks between the terrestrial carbon cycle and climate, which remains one of the largest uncertainties in current projections of future climate (Dorrepaal et al., 2009). Northern Peatlands are the long-term sink of atmospheric carbon dioxide (CO<sub>2</sub>) (Gorham, 1991; Turunen et al., 2002) containing one-third of the world's soil organic carbon, equivalent to more than half the amount of carbon in the atmosphere (Gorham, 1991). Peatlands occupy approximately 12% of Canada's land area with the vast majority (97%) occurring in the subarctic boreal region (Tarnocai, 2006). Peatlands are implicated in the surface-atmosphere exchanges of mass and energy (Hinzman et al., 2005), greenhouse gas fluxes (Prowse and Frugal, 2009; Schuur et al., 2015), water distribution (Connon et al., 2014) and ecologic responses (Baltzer et al, 2014). The carbon-sink net capacity of peatlands is primarily controlled by the water table position (Gorham et al., 1991) as well as the long mean residence times of water in these ecosystems (Waddington et al., 2010). Lateral water flow in peatlands is controlled by their low hydraulic gradients and the steep decline (3-5 orders of magnitude) in hydraulic conductivity with depth (Whittington and Price, 2006).

Understanding the thermal regime of the soil profile, as well as freezing and thawing dynamics in the context of climate change is crucial in many scientific and engineering applications. Freezing and thawing in soils are highly non-linear processes that depend on strongly coupled hydrologic and thermal processes. These processes are coupled through the phenomena of phase change, cryosuction, advective heat transport, thermal conductivity dependence on frozen and unfrozen moisture content, dissolved ion concentration, and hydraulic conductivity dependence on ice content. The physical characteristics of peat that could affect

their energy budgets (e.g., density, water-holding capacity) are a direct reflection of biotic processes, i.e. plant species composition, net primary productivity and decomposition dynamics, demonstrating a significant biotic control over internal thermal conditions as a short-term response of peatlands to climate change (Bridgham et al., 1995).

Snow is a critically important cryogenic element of the northern environments (Mellander et al., 2007). It has a powerful effect on the soil thermal regime depending on many factors such as precipitation patterns within the season, snow cover depth, density, structure and duration on the ground (Zhang, 2005). Its thermal and optical properties control local energy regimes and can substantially influence the fate of permafrost (Zhang and Armstrong 2001).

Snow cover, stratigraphy and physical properties are naturally changing throughout the season as a result of climate driven metamorphosis (Pomeroy et al., 2001) however, how these natural processes are likely to be affected by climate warming and their impacts on the environment are poorly understood. Climate warming increases the likelihood of unseasonal thaws, later onset of snow cover, early snowmelt, consequent decreased duration of the snow-covered period (Derksen et al., 2012), and rain on snow events (Liston and Hiemstra, 2011). These changes impact snow properties and runoff (Semmens and Ramage, 2013) and because of their importance to soil energy budget and to thermal gradients between soil and atmosphere, they are critically important for the energy balance of these environments. A big challenge in evaluating these changes and understanding their impacts arises from the fact that changes in snow properties are not uniform across the boreal/subarctic region, and the affected processes function and respond at different temporal and spatial scales (Bokhorst et al., 2016).

The effects of climate change in the northern environments are further exacerbated by anthropogenic disturbance such as pipelines, winter roads and seismic lines. Those expansive disturbances are related to past resource exploration however, other forms of exploration and development are expected in the future. The total length of winter roads and seismic lines within the Scotty Creek basin (which covers 152 km<sup>2</sup> and where Scotty Creek Research Station is located, and this study was conducted) has been estimated at 133 km, which is over five times the natural drainage density of the basin (Quinton et al 2011), indicating its implication in the hydrology of the basin. Seismic lines are the most widespread type of human disturbances in northern environments. They cut continuously through various terrain types and have been shown to have a detrimental effect on permafrost (Braverman and Quinton, 2016). The incision of the seismic line involves sequential processes of canopy removal (MacFarlane 2003), increased solar radiation (Revel et al., 1984), ground compaction and subsidence (Haag and Bliss, 1974). Those initial ecosystem changes result in feedback mechanisms promoting permafrost thaw, increased hydraulic conductivity and soil moisture content (Jorgenson et al., 2010), consequent heat and mass transfer and resulting in further permafrost degradation (Braverman and Quinton 2017).

The recovery of the seismic lines depends primarily on the latitude of its occurrence and the severity of the initial disturbance (Williams et al., 2013) following the trend of increasing recovery time with decreasing duration of the vegetative season. Site-specific observations suggest the “drifting” of the seismic lines as a result of localized simultaneous permafrost aggradation on the south-facing slopes and degradation on the north-facing slopes. Localized conditions can facilitate permafrost aggradation owing to the insulating properties of dry peat.

However, it is important to note that net permafrost loss associated with seismic lines appears to be irreversible due to positive feedback mechanisms.

Mechanical ground cooling approaches have been investigated in mineral-based substrates with many successful outcomes, however, in peat-based environments they remain largely unexplored. Ground cooling systems are used in application-oriented projects largely pertaining to civil engineering operations. As such, their use in the remote wetland environments range from minimal to non-existent. However, fast rates of climate change and concomitant landscape evolution coupled with increasing socio-economic activity in the far North affirm the growing need for the advancement of ground-cooling technologies in peat-based substrates.

This research seeks to advance the understanding of the ground cooling systems in a peat-dominated environment through an overarching research question: What is the most efficient cooling system in a highly saturated peatland environment? This question was addressed by analyzing the annual ground temperature profiles and the vertical and horizontal extent of freezing front propagation for various systems. This investigation was conducted in three stages and although not all factors have been explored exhaustively due to the limited scope of this investigation, the foundation for further work has been established.

In the first stage of the investigation the main attributes of interest were physical properties of the thermosyphon operating fluids (single-phase versus two-phase), and principles of operation (passive versus active). Three systems were compared in a semi-qualitative manner. The initial phase of development commenced with an installation of double-phase, passive design in multiple configuration (7), which was later replaced with individual single-phase active design followed by single-phase, active design in multiple configuration (4). Each subsequent

design was determined based on the semi-qualitative data assessment, i.e. the effects of each attribute were not systemically compared amongst each design, rather ground temperature changes generated by each design were assessed.

The second phase of the investigation evaluated the effects of snow on the ground thermal regime as well as on the single-phase, active thermosyphon. Single-phase, active model was selected because it has been determined to be more efficient at heat transfer than the two-phase passive design which justified further upgrade investigation. 4 equivalent snow shading cones were installed at different locations along the seismic line representing sites of lower and higher saturation.

In the third phase two single-phase, passive coaxial designs were compared: with and without inner pipe insulation, to investigate the lateral thermal gradients within the thermosyphon and the concomitant overall efficacy.

The key research objectives of this study were to:

- Evaluate the performance of three ground cooling systems installed at Scotty Creek Research Station, NT, between 2013-2017. These systems are: (1) two-phase, passive, 7-thermosyphon configuration (**two-phase, passive7**), (2) single-phase, active thermosyphon (**single-phase, active1**) and (3) single-phase, active, 4-thermosyphon configuration (**single-phase, active4**)
- Evaluate the insulating effect of snow on the ground thermal regime along the seismic line by removal and reduction of the snowpack using four individual snow-shading cones (2018)

- Investigate the combined cooling efficiency of a single phase, active thermosyphon conjoined with a snow shading cone (**single-phase, active with cone**), (2018)
- Compare the performance of two systems, installed in 2019. These systems are: (1) single-phase, passive, coaxial, non-insulated thermosyphon (**non-insulated coaxial**) and (2) single-phase, passive, coaxial, insulated thermosyphon (**insulated coaxial**). This assessment was preliminary and requires further investigation.

## **Chapter 2: An evaluation of ground-freezing methods at Scotty Creek Research station in the zone of discontinuous permafrost, Northwest Territories**

**ABSTRACT:** Northwestern Canada is one of the most rapidly warming regions on Earth. The southern limit of the discontinuous permafrost zone is highly sensitive to small climatic fluctuations and presently experiencing a rapid landscape change due to accelerated permafrost thaw, which is further exacerbated by anthropogenic disturbances such as seismic exploration. Recent research has begun to examine both natural and mechanical approaches to minimize permafrost loss, although the utility of such methods in peatland environments is not well understood. This study explored the efficiency of natural and artificial ground cooling processes in a peatland environment by evaluating snow exclusion and thermosyphon methods. Ground-freezing devices have been used at the Scotty Creek Research Station in the Northwest Territories, Canada, since 2013 for experimental studies on permafrost stabilization and regeneration. Data arising from these studies were used in the present study to evaluate the effectiveness of specific designs and applications of such devices. The effect on ground freezing was evaluated for 7 freezing systems deployed along the seismic line: (a) two-phase, passive, 7-thermosyphon configuration, (b) single-phase, active thermosyphon, (c) single-phase, active, 4-thermosyphon configuration, (d) single-phase, passive, coaxial, non-insulated thermosyphon, (e) single-phase, passive, coaxial, insulated thermosyphon, (f) single-phase, active thermosyphon conjoined with the snow shading cone and, (g) four individual snow shading cones. It was found that the single-phase, active thermosyphon conjoined with the snow shading cone was the most effective ground freezing system in a highly saturated peat environment, reaching minimum

ground temperatures between -13.3 to -14.2 °C 80 cm below the ground surface. Natural ground cooling by direct coupling of air and ground temperatures is strongly limited by the presence of snow however, average ground temperatures in the snow-reduced areas remained lower by only 0.7-1.2 °C within an 80 cm vertical profile than in the snow-covered areas, which suggests that other factors such as moisture content may exert dominant control over ground cooling range. Nonetheless, at the end of the summer snow-reduced areas maintained a 15 cm thick frozen layer at 60 -75 cm below the ground surface. We are proposing that systematic monitoring of snowpack development and decay can be used as a proxy for ground thermal profile evaluation. This study supports the feasibility of low cost, readily deployable ground freezing systems that can mitigate permafrost thaw and improve the adaptability of engineering designs to changing environmental conditions.

## 1. Introduction

Northwestern Canada is one of the most rapidly warming regions on Earth in recent decades (Jones and Moberg 2003; Smith and Reynolds 2005; Vose et al. 2005) with significant impacts on terrestrial and aquatic ecosystems. This has led to unprecedented permafrost thaw (Oberman et al., 2001; Schuur and Abbott, 2011) and permafrost thaw-induced land cover changes, catalysing extensive research on the causes, mechanisms, rates and patterns of coupled permafrost thaw and the resulting land cover changes. Permafrost thaw is one of the most obvious indicators of climate change (Burgess et al., 2000), triggering considerable land cover (Haynes et al., 2018) and hydrological (Williams et al., 2013; Kurylyk et al., 2016;) changes. The thaw of ice-rich permafrost invariably results in ground surface subsidence which threatens the structural integrity of infrastructure with resulting negative socio-economic consequences (Davidson et al., 2003). The southern limit of discontinuous permafrost, where permafrost is typically isothermal at the melting point temperature throughout its 10-15 m thickness (Kwong and Gan, 1994), is especially sensitive to small climatic fluctuations and it has been consequently degrading as a result of increasing rates of warming in this region (Quinton et al., 2009).

Sustained permafrost thaw is a clear indication of a warming climate (Goodison and Walker, 1993). In the northern hemisphere, permafrost thaw-induced land cover change is especially pronounced between the latitudes of 59° N and 62° (Johannessen et al., 2004; Akerman and Johansson, 2008; Romanovsky et al., 2010; Quinton et al., 2011; Beck et al., 2015). Predicting the impacts of climate warming on permafrost is complicated by the poor understanding of possible feedbacks with other ecosystem components. An approximate

indicator of permafrost presence is the average annual air temperature below 0° C (Halsey et al., 1995). On a large continental scale, increasing mean annual air temperatures (MAAT) are the leading cause of permafrost degradation (Osborne et al., 2018). At the synoptic scale, an increased occurrence of warm air masses over permafrost terrains contributes to local surface energy balances through regional advection. However, other localized conditions, such as soil moisture, ground surface albedo, vegetation, and ground heat fluxes (Smith, 1975; Smith and Riseborough, 1983) influence local energy balance and therefore play an important role in permafrost sustenance. For example, dry peat is an extremely effective thermal insulator (Beilman et al., 2001; Turetsky et al., 2007) and dry peat-covered surfaces that predominate in the southern margin of discontinuous permafrost (Kwong and Gan, 1994) thermally insulate the underlying permafrost even where the MAAT exceeds 2° C (Camill, 1999). The rates of permafrost thaw are often greatest where in addition to the above processes, warming of the ground is augmented by anthropogenic disturbance, such as the roads, seismic lines and pipelines and other infrastructure (Reynolds, et al., 2014).

There is a growing need for knowledge-based tools and methods to mitigate permafrost thaw meant for both mitigation strategies and engineering designs in their adaptability to a wide range of changing environmental conditions. Thermosyphons are the most widely used devices to prevent the thaw of permafrost, the designs of which vary to suit specific applications including stabilization of building foundations (Popov et al., 2010), road and rail embankments (Zarling and Brayley, 1987; Forsstrom et al., 2002; Wen et al., 2005; Xu and Goering, 2008), containment of contaminants (Edlund et al., 1998; Hayley et al., 2004) and preservation of archeological or other culturally significant sites (Goetz, 2010). The fundamental physical phenomenon governing the functionality of a thermosyphon is the spontaneous heat

exchange due to the temperature gradients between the soil and the thermosyphon and the thermosyphon and the atmosphere, making it a convective device which extracts heat from the ground and discharges it to the atmosphere (Long and Zarling 2004). Although substantial progress has been made in thermosyphon research and development, their effectiveness in peat-based environments is not well understood.

Development of the most efficient designs for remote peatland environments must address three main challenges: the exposure to the extreme temperatures, high moisture saturation of the ground profile and prolonged periods between maintenance. Considering climate warming in northern environments, changes in local climatic variables which might affect permafrost must also be considered. Snow cover has a powerful effect on soil thermal regime depending on many factors such as precipitation patterns, snow cover depth, type, and duration on the ground (Zhang, 2005), essentially enabling it to insulate the ground from heat fluxes due to its extremely low thermal diffusivity (Goodrich, 1982). Both local and large-scale climatic responses are a direct consequence of the change in the land surface energy balance, which is influenced by the presence of snow, with fall precipitation being the primary control.

Thermal and optical properties of snow control local energy regimes and snowpack presence is therefore greatly implicated in the overall permafrost stability. The temperature of the snow at the snow-atmosphere interface is relatively low due to high albedo, emissivity and exposure to wind (Cline, 1997; Marshall et al., 2003; Zhang, 2015). The extremely low thermal diffusivity of the snowpack due to its high air content restricts the diffusive heat fluxes from the ground to the atmosphere (Cohen, 1994). As a result, permafrost tends to be warmer in areas of higher snow accumulation and becomes more susceptible to temperature changes and consequent degradation (Jafarov et al., 2018). Snow cover, stratigraphy and physical properties are naturally

changing throughout the season as a result of climate-driven metamorphosis (Pomeroy and Brun, 2001), however, these natural processes are likely to be affected by climate warming and the implications on ground thermal regime and permafrost stability has not been exhaustively explored.

This study aimed to increase the understanding of the efficacy of ground cooling systems designed to stabilize permafrost in a peatland-dominated region of thawing, discontinuous permafrost. The overarching research question was: What is the most efficient design in a highly saturated peatland environment?

This investigation was conducted in three stages which addressed the following considerations. In the first stage of the study the two-phase, passive models were installed which were later replaced by a single-phase model with enhanced circulation (active), followed by a cluster of four single-phase, active thermosyphons. During this stage it was determined that operating fluids in two-phases are less efficient at heat transfer than in a single phase. Although the individual effects of physical properties of the operating fluids (two-phase) and principles of operation (active) on heat transfer were not decoupled in the single-phase, active thermosyphon, the results established a rational direction for the advancement of the models.

The second phase of the investigation evaluated the effects of snow on the ground thermal regime as well as on the single-phase, active thermosyphon. This model was selected because it has been determined to be more efficient at heat transfer than the two-phase passive design which justified further upgrade investigation. It was conjoined with the snow shading cone to reduce the insulating effect of snow. 4 equivalent snow shading cones were installed at different locations along the seismic line representing sites of lower and higher saturation.

In the third phase two single-phase, passive coaxial designs were compared: with and without inner pipe insulation to investigate the lateral thermal gradients within the thermosyphon and the concomitant overall efficacy.

The specific objectives of this study were to: (1) assess the efficiency of 5 thermosyphon designs and configurations along the seismic line: a) **two-phase, passive**, b) **single-phase, active**, c) **single-phase, active**, d) **non-insulated coaxial**, and e) **insulated coaxial**; (2) evaluate the insulating effect of snow on the ground thermal regime along the seismic line by removal and reduction of the snowpack; and to (3) investigate the combined cooling efficiency of a single phase thermosyphon conjoined with a snow shading cone (**single-phase, active with cone**).

## 2. Study Site

The Scotty Creek Research Station (61.18°N, 121.18°W) is located approximately 50 km south of Fort Simpson, NT, and it is situated at the southern limit of the zone of sporadic-discontinuous permafrost within the Scotty Creek watershed (Figure 1a). The watershed covers a 152 km<sup>2</sup> area in the lower Liard River valley (Figure 1b). The headwaters of the Scotty Creek watershed are characterized by upland moraines (48%), raised permafrost plateaus (20%), ombrotrophic bogs (19%), channel fens (12%), and lakes (2%) (Chasmer et al., 2014). In this zone, permafrost thickness is on the order of 10 m (Burgess and Smith, 2000), isothermal around 0°C (Kwong and Gan, 1994), and remains relatively warm throughout its thickness, emphasizing susceptibility to climate change.

The area of the Scotty Creek Research Station comprises three main land cover types closely related to permafrost distribution (Quinton et al., 2009). These landcover classes are:

(1) forested peat plateaus underlain by permafrost, elevated approximately 1-2 m above the surrounding wetland and dominated by black spruce trees (*Picea mariana*), ericaceous shrubs (e.g. *Rhododendron groenlandicum*), lichens (*Cladonia spp.*), and mosses (*Sphagnum spp.*); (2) ombrotrophic bogs- permafrost-free water storage features varying in size and level of connectivity, dominated by mosses (*Sphagnum balticum* and *S. magellanicum*); (3) riparian channel fens- permafrost-free drainage corridors, dominated by sages (*Carex spp.* and *Eriophorum spp.*) (Garon-Labrecque et al., 2015). Peat deposits in this region range from 2-8 m in thickness and overlie a silty-clay to clay-rich glacial till (Connon et al., 2015; McClymont et al., 2013). All three land cover types have distinct thermal and hydrological regimes and play important roles in routing water through this environment. The wetland is also affected by anthropogenic impacts, which influence the hydrologic network. There are two seismic lines dating back to the 1960s and 1980s and two winter roads incised through the landscape (Figure 1c). Their level of post disturbance recovery varies. Permafrost thaw in this region has been very rapid (Robinson & Moore, 2000); in 1947 it occupied approximately 70% of the Scotty Creek headwater area but had decreased to approximately 43% by 2008 (Quinton et al., 2011). As the permafrost below plateaus thaws, the plateau ground surface subsides and becomes inundated by the adjacent wetlands. This process results in the conversion of forest to wetland (Lara et al., 2016; Quinton et al., 2011; Zoltai, 1993).

A section of seismic line approximating 500 m in length was used for this study (Figure 1c), representing a linear disturbance on various landcover types. Two thermosyphon experimental sites were established: East site and West site, with an approximate distance of 200 m between them. Four additional locations were selected for the stand-alone snow shading cones which controlled snow accumulation patterns on the ground (Figure 1c).

East site was established in 2013, approximately in the middle of the seismic line that traverses a peat plateau, approximately 100 m from the fen (Figure 1c). The area was vegetated by a mixture of mosses (*Sphagnum spp.*), shrubs (*Rhododendron groenlandicum*), lichens (*Cladonia spp.*), and some sparse tree seedlings (*Picea mariana*). It exhibited early stages of vegetation recovery as evidenced by the presence of hummocks facilitating germination and subsistence of shrubs and tree seedlings.

The vegetation recovery of the seismic line in the East-West direction appears as a gentle meandering of the seismic line which, when first incised, was a straight line. However, seismic lines are highly dynamic pathways for subsurface water flow (Braverman and Quinton, 2015) and therefore permafrost recovery in the East-West direction is highly unlikely. There are isolated areas on the south facing slopes of the seismic line (North-South direction) which facilitate localised aggradation of permafrost owing to high insulating properties of dry peat. However, because this aggradation is site specific and the stability of the new formed permafrost is not exhaustively explored, it does not constitute the recovery of the seismic line on a larger spatial scale.

East site is typically fully saturated at the end of the summer season with the water table at approximately ground surface level. No permafrost was detected with a 1.5 m probe within 2 m radius of the experimental setup at the end of August 2018. The designs installed on East site between 2013 and 2019 were: (a) two-phase, passive, 7-thermosyphon configuration, (b) single-phase, active thermosyphon, (c) single-phase, active, 4-thermosyphon configuration, (d) single-phase, passive, coaxial, non-insulated thermosyphon, and (e) single-phase, passive, coaxial, insulated thermosyphon.

West site was established in 2018, approximately 200 m west from the East site, on the elevated north edge of the seismic line adjacent to the peat plateau. This site was selected due to the closed talik present on the edge, which was connected to the suprapermafrost lateral talik of the lower in elevation central channel of the seismic line. The design installed on West site was the single-phase, active thermosyphon conjoined with the snow shading cone. The combination of the site elevation of the north edge of the seismic line (approximately 50 cm above the central channel of the seismic line) and the south-facing orientation was conducive to drainage and desiccation of the top peat layer. In late August 2018 permafrost table was recorded with the 2 m permafrost graduated probe at 137 cm below the ground surface and water table was at 70 cm below the ground surface delineating a 67 cm thick saturation zone. Vegetation was of the same composition as at the East site but with a higher concentration of lichens (*Cladonia spp.*). When dry, highly porous peat adopts extremely low thermal diffusivity of air and becomes a very effective insulating agent (Moore, 1987), however, proximity to the seismic line promotes talik formation within peat plateaus due to the high saturation of the seismic lines which are acting as water channels and consequently supply a lot of heat to the adjacent plateaus through advection (Braverman and Quinton, 2015). At West site the combined effects of subsurface water flow and preferential snow accumulation resulted in the formation of a talik, which was approximately 3 m long, 2 m wide and 1.6 m deep.

Cone1 was situated at the centre of the seismic line transecting a plateau, about 20 m west from the fen. The vegetation was dominated by mosses (*Sphagnum spp.*) and shrubs, predominantly Labrador Tea (*Rhododendron groenlandicum*). Some hummocks and irregularly scattered seedlings of black spruce (*Picea mariana*) were present indicating a degree of recovery of the seismic line; however, no permafrost was detected with a 1.5 m probe. Depth to the water

table was approximately 18 cm below the ground surface at the end of August 2018. Cone2 was also located in the middle of the seismic line adjacent to the peat plateau, about 30 m west from Cone1. Depth to the water table was approximately 23 cm below the ground surface at the end of August 2018 and there was a mature tree (*Picea mariana*) located approximately 60 m northeast. At the northeast edge of the cone isolated permafrost patch was detected at 62 cm below the ground level (proximity to the tree), everywhere else at this location it was undetectable with a 1.5 m probe. Cone4 was located on the north-facing slope of the seismic line about 25 m west from West site. The vegetation included shrubs, predominantly Labrador tea (*Rhododendron groenlandicum*), lichens (*Cladonia spp.*) and small black spruce tree seedlings (*Picea mariana*). Isolated permafrost patch was detected 70 cm east from the cone, at 80 cm below the ground surface, whereas everywhere else within a 2 m radius from the experimental setup it was undetectable with a 1.5 m probe. Water table was non-discernible. Isolated patches of permafrost at Cones 2 and 4 are most likely due to the sparse raised hammocks overlaid with dry peat which acts as an efficient insulator. Cone5 was located at the south-facing edge of the seismic line adjacent to the bog, approximately 150 m west of Cone4. No permafrost was detected with a 1.5 m probe. This site was dominated by mosses (*Sphagnum spp.*) and sporadic sedges (*Cyperaceae spp.*) Depth to the water table was approximately 15 cm below the ground surface at the end of August 2018.

### **3. Methods**

#### **3.1 Thermosyphons-Design Evolution**

The purpose of a thermosyphon is to increase the rate of heat loss from the ground. At Scotty Creek, numerous designs and installation configurations have been examined for their

efficacy in this environment (Figure 2a). The general considerations for the thermosyphon design include physical principles governing heat transfer, types of operating substance and mechanical principles of operation (Figure 2b). The combination of extreme seasonal climatic conditions at Scotty Creek as well as logistical and maintenance challenges during parts of the year have propelled the expansion of thermosyphon designs. The ongoing goal is to develop a design that will integrate and optimize performance efficiency, durability and cost considerations.

Thermosyphon research at Scotty Creek was launched in 2013 at East site with the installation of the two-phase, passive, 7-thermosyphon configuration (**two-phase, passive7**) along the southern edge of the seismic line adjacent to the peat plateau (Figure 3a). Two-phase thermosyphon operates under the principle of phase change of the working fluid and the concomitant heat transfer. The basic design of a two-phase thermosyphon typically consists of a closed-ended tubular vessel partially filled with a working fluid. The vapor phase of the working fluid fills most of the interior of the vessel, with the liquid phase filling the minority (Figure 3b). Each thermosyphon of the original design consisted of a 6.10 m aluminum tube with the interior diameter of 7.6 cm and a wall thickness of approximately 3 mm. Both ends were capped with rigid plastic caps and sealed with silicon sealant. The tubes were filled with isopropyl alcohol up to 10 cm in height. Thermosyphons were installed on top of the permafrost which ranged between 180-218 cm from the ground surface, with the average distance of 200 cm from the ground surface. Eight thermistor sets (Campbell Scientific 109 series) were installed adjacent to the thermosyphons (Figure 3a) (red circles). All thermistors used in this study had a  $\pm 0.2$  °C margin of instrumental error. The distance between thermistors and the nearest thermosyphons ranged between 14-26 cm, with an average length of 20 cm. Thermistors were attached to plastic poles, which were inserted into the ground. Each pole had three thermistors attached to it at 5, 10

and 15 cm from the bottom of the pole, their distance from the ground surface was 185, 190 and 195 cm. All data was recorded using Campbell Scientific dataloggers (CR Series) with a measurement interval of 60 seconds and averaged data output every 30 minutes.

In August of 2016 one of the original thermosyphons (6) was replaced with a single-phase, active design (**single-phase, active1**). The 3.05 m aluminum tube was filled up with a glycol-based coolant (commercial antifreeze), resulting in a single-phase thermosyphon. At the bottom of the pipe a mechanical pump was installed to increase the circulation rate of the coolant (Figure 4). This design operated under the physical principle of thermal diffusion (Soret Effect) propelled by temperature driven density changes of the coolant (Rahman and Zagher, 2014) and radiative heat transfer to the atmosphere. The differential temperature and density of the fluid within the pipe induce convection which is greatly enhanced by the addition of a pump, consequently enhancing the rate of heat transfer, which is directly proportional to fluid velocity.

In August of 2017 three more thermosyphons (4, 5 and 7) were replaced with a single-phase, active design equipped with an upper pump, creating a 4- single-phase thermosyphon configuration (**single-phase, active4**). The installation of the pump at the upper section of the thermosyphon allowed for the ease of access and maintenance. In August of 2018, at the West site a single-phase, active thermosyphon equipped with an upper mechanical pump and the snow shading cone was installed (**single-phase, active with cone**) (Figure 7b). The purpose of the snow shading cone was to prevent the accumulation of snow at the ground surface. The thermosyphon consisted of a 3.05 m aluminum tube with the interior diameter of 8.2 cm and the outside diameter of 8.9 cm. Both ends were capped with rigid plastic caps and sealed with silicon sealant. The tubes were filled with glycol-based coolant (commercial antifreeze) up to approximately 20 cm from the top ridge. The base of the thermosyphon was installed on top of

the permafrost at approximately 137 cm below the ground surface. The snow shading cone was made of galvanized stainless steel. It had a diameter of 1m and was mounted on top of the thermosyphon, approximately 50 cm above the ground, with the thermosyphon passing through the top opening of the cone (Figure 5a). 3 sets of thermistors were installed at the experimental site (Figure 5b). All thermistors were attached to the plastic poles which were inserted into the ground. 5 thermistors (Campbell Scientific 109) were installed at the thermosyphon wall (A) at depths of 5 cm, 25 cm, 50 cm, 70 cm and 80 cm from the ground surface (Figure 5b). This set was monitoring the vertical ground temperature profile adjacent to the thermosyphon within the seasonally frozen layer range. Another set of thermistors (Campbell Scientific 109) was installed approximately 25 cm away from the thermosyphon (B), at 5 cm, 25 cm, 50 cm, 100 cm, 120 cm, 130 cm and 140 cm from the ground surface. This thermistor set was installed to monitor the vertical ground temperature profile under the cone but at a distance from the thermosyphon wall. A pre-existing set of thermistors (Campbell Scientific 109) at depths of 10 cm, 50 cm, 75 cm, 100 cm and 145 cm from the ground surface (C), approximately 100 cm away from the snow shading cone was considered the control site (Figure 5b). All data were recorded using Campbell Scientific dataloggers (CR200) with a measurement interval of 60 seconds and averaged data output every 30 minutes. The site was equipped with the wildlife camera (Reconyx UltraFire Xr6 Covert IR Game Camera) to monitor snow accumulation patterns.

At the beginning of February 2019 two new single-phase thermosyphon designs were installed on East site: single-phase, passive, insulated coaxial and single-phase, passive, non-insulated coaxial (**insulated coaxial**, and **non-insulated coaxial**). Each consisted of a coaxial pipe 3 m in length. The diameter of the external aluminum pipe was approximately 7.6 cm and the diameter of the internal PVC pipe was approximately 2.5 cm. The internal pipe featured 5 cm

parallel slots at the bottom. Both thermosyphons were filled with glycol-based cooling liquid (commercial antifreeze). The insulated co-axial design had foam insulation secured with adhesive tape around the interior pipe, while the non-insulated co-axial design was insulation-free (Figure 6a, b).

Both designs were passive and operated under the physical principle of thermal diffusion (Soret Effect) and radiative heat transfer. In these designs the cooled, dense liquid sinks to the bottom of the tube along the walls of the outer tube displacing the warmer fluid through the grooves of the inner tube (Figure 6). Insulation of the inner tube in the insulated coaxial design facilitates larger lateral thermal gradient between the liquid in the inner tube and outside of it, allowing for more efficient gravitational cycling and heat transfer to occur throughout the winter season than in the non-insulated coaxial. In the absence of insulation some of the heat is lost from the inner tube to the liquid outside of it and the lateral heat gradient is lowered. Conversely, both systems deactivate when subsurface temperatures are lower than the air temperature and below ground cooling liquid is cool and dense. Each thermosyphon had a set of thermistors (Campbell Scientific CR series) attached outside of the exterior thermosyphon tube at the ground surface, at 25 cm, 50 cm, 75 cm, 100 cm, 125 cm and 150 cm below the ground surface. All data were recorded using Campbell Scientific dataloggers (CR300) with a measurement interval of 60 seconds and averaged data output every 30 minutes.

### **3.2 Snow Exclusion Experiment**

Four stand-alone snow shading cones were installed along the seismic line at four sites (Figure 1c). The cones were designed to prevent snow build-up on the ground directly under them. The snow was deposited on the sides of the cones but in two instances (Cones 1 and 5) it

eventually covered the opening to the atmosphere and prevented air circulation, essentially decoupling temperatures outside and under the cones. Each cone was custom made with galvanized stainless steel. The cone diameter and height were 1 m and 0.6 m respectively. The top of each cone had a 10 cm opening to allow air circulation and a smaller cone with a 25 cm diameter was attached above it on a round steel frame to prevent snow accumulation under the cone through the top opening (Figure 7a). The average distance between the ground and the cone base was approximately 50 cm. A pre-existing set of thermistors, located approximately 1 m from the snow shading cones, was present at each site. The installation of the original thermistor sets was contingent on the past permafrost presence, therefore the depths differed from the sets installed for the snow shading experiment, which targeted upper layer of the soil profile at 5 cm, 25 cm, 50 cm, 70 cm and 80 cm below the ground surface. Intra-site assessment of both sets of thermistors was evaluated based on depth compatibility. The locations of the snow-shading cones were selected to represent natural spatial variability observed along the seismic line including differences in aspect (north-facing, south-facing and centrally located), topographic position and proximity to adjacent wetlands. Cone5 was equipped with the wildlife camera (Reconyx UltraFire Xr6 Covert IR Game Camera) to monitor snow accumulation patterns and snow drift since this was a relatively open location compared to other sites. There was a pre-existing set of temperature sensors (Campbell Scientific SR50) outside Cone5, located at the ground surface and at 10 cm, 30 cm and 50 cm above. This set was used as a proxy to estimate snow depth at Cone5, as proposed by Danby and Hik, 2007. This method compares temperature measured in the atmosphere and beneath the snow surface. When the atmospheric temperature (measured at the Fen MET station) was comparable with the temperature at a given sensor (within 2 °C) the inference was made that there was no snow at that height, according to the

method proposed by Lewkowicz, 2008. The results were confirmed by digital images taken by the wildlife camera which captured the sensors and snow cover development relative to them. On 3 February 2019 accumulated snow was assessed and systematically removed from each cone and within 1 m radius of the rim.

### **3.3 Assessment of the simple 1-D heat conduction model (Braverman) and freezing front development analysis**

A 1D Heat Conduction Model (Braverman, Personal Communications, 2017) was used to evaluate the depth of frozen ground under cones 1 and 2. The model computes the temporal and spatial (1D) progression of 0 °C isotherm (corrected for zero-point depression of -0.2 °C) as a function of heat transfer, which is controlled by soil properties, boundary conditions and atmospheric forcing. The zero-point depression value varies between -0.14 °C and -0.24 °C, as proposed by Quinton et al., 2005, and depends on water content, soil matrix (porosity) and water chemistry.

## **Results and Discussion**

### **4.1 Thermosyphons**

#### **4.1.1 Two-phase, passive<sup>7</sup>**

The control site outside of the experimental setup recorded average ground temperature of 0.1 °C at 2.0 and 2.5 m for 3 consecutive winters which is typical for this type of terrain (Tarnocai and Stolvoboy al., 2006). The original configuration of 7 two-phase thermosyphons did not yield any significant temperature decrease during the winters of 2013 to 2015 (Figure 8) and the temperatures between 2.2-2.4 m depth remained at approximately 0 °C ( $\pm 0.2$  °C). This is

likely the result of a very low latent heat exchange rate (44.0 kJ/mol) and low heat capacity (0.58 kcal/kg C at 10 °C) of isopropyl alcohol, which resulted in small temperature gradients between the liquid phase in the thermosyphon and the adjacent ground. A larger volume of isopropyl alcohol would have increased the efficiency of heat transfer. Additionally, the possible formation of homogenous, binary mixture of isopropyl alcohol and water in the vapour or liquid phase might have contributed to the lower heat exchange rate between the thermosyphon system and the surroundings. Although at the time of installation the tube was capped and sealed, it is very likely that over time it became permeable to air which was the source of water.

#### **4.1.2 Single-phase, active1**

In February 2017, six months after the installation of single-phase, active1 the temperature at 0.25 m from thermosyphon 6 was approximately -1.0 °C ( $\pm 0.2$  °C), (Figure 8) at depths of 2.2-2.4 m. Thermistors outside of the experimental set-up recorded the temperature of -0.1 °C ( $\pm 0.2$  °C) and there was a comparable snow cover present in both years. It is noteworthy that the temperature remained at approximately 0°C during the following summer, whereas in the preceding years it peaked on average at approximately 1.5 °C (Figure 8). These results showed that single-phase, active design was more effective than the two-phase, passive design. The enhanced convection and a more efficient latent heat exchanges of the operating substance (glycol-based antifreeze) are the likely causes.

#### **4.1.3 Single-phase, active4**

In August 2017 the configuration expanded to four (three more replaced from the original single-phase7 configuration) with the pump installed at the upper section of the tube in each thermosyphon. In December 2017 ground temperatures at depths between 2.2 and 2.4 m further

decreased to approximately  $-2.0\text{ }^{\circ}\text{C}$  ( $\pm 0.2\text{ }^{\circ}\text{C}$ ), (Figure 8), suggesting a synergistic cooling effect. As temperature gradients were created, heat fluxes increased leading to lower ground temperatures. The installation of the upper pump allowed for expedient accessibility and maintenance.

#### **4.1.4 Single-phase, active with a cone**

The purpose of a single-phase, active, pump-operated thermosyphon conjoined with a snow-shading cone (installed in the fall of 2018) was to explore the combined effects of forced convection (pump-enhanced movement of heat-carrying liquid) and the absence of snow insulation on ground cooling. Temperature time series were analyzed for three sets of thermistors: at the tube (A), 25 cm away from the tube (B) and outside of the experimental area, approximately 1 m away from the snow-shading cone (Figure 5b). There was a period of battery failure and consequent pump shut down estimated for December 2018 and January 2019. The design failed to provide consistent snow-free area and by the end of December ground surface under the cones was thoroughly insulated.

Considering those circumstances, the data were analysed in relevant intervals: from the installation till the end of November (pump and snow-free, as determined by the images from the wildlife cameras) (Figure 9c); December (no pump but ground remained snow-free)(Figure 9d); January (no pump and snow insulation)(Figure 9e); February and March (pump reactivation and snow removal)(Figure 9f, g). From the onset of consistent sub-zero  $^{\circ}\text{C}$  temperatures within the soil profile at the end of October, 2018 until mid April, 2019 the temperature patterns at each depth were similar and the averaged magnitude variations between 5 depths (5 cm, 25 cm, 50 cm, 70 cm and 80 cm) were  $0.4\text{ }^{\circ}\text{C}$  indicating consistency of heat transfer along the tube (Figure

9a). In mid November the temperatures along the tube reached a range of  $-6^{\circ}\text{C}$  to  $-7.3^{\circ}\text{C}$ . In December the ground under the thermosyphon remained only partially snow-covered which allowed for air circulation under the cone.

Despite the pump shut-down during the month of December, there was a decreasing ground temperature trend as evidenced by the slope of the line of best fit:  $y = -0.1249x + 5422.7$  (Figure 9d) due to combined effects of natural convective heat transfer within the thermosyphon and ground heat loss through the snow-free surface. In December the lowest ground temperatures reached a range of  $-7.4^{\circ}\text{C}$  to  $-8.3^{\circ}\text{C}$ . In January the ground became insulated by snow and although at the beginning of January the temperatures decreased to the range of  $-8.3^{\circ}\text{C}$  to  $-9.3^{\circ}\text{C}$  the rate of heat transfer was impeded as evidenced by the slope of line of best fit  $y = -0.0767x + 3327.5$  (Figure 9e). At the beginning of February, the snow was removed from around the cone (approximately 70 cm in depth) and the pump was reactivated. Within two days, the temperatures reached their minimum seasonal values in the range of  $-13.3^{\circ}\text{C}$  to  $-14.2^{\circ}\text{C}$ . These findings emphasize the implication of snow in the efficacy of ground cooling systems and can inform future installation considerations for individual projects. We also hypothesize that snow compaction due to in-situ investigative activity in February 2019 increased thermal conductivity, which might have contributed to increased rates of ground cooling. The thermal conductivity of snow varies mostly with density, but also with crystalline structure and grain to grain contact. When compacted, air is forced out of the snow matrix and it becomes denser with higher ratio of grain to grain contact, allowing for the ground heat to be conducted more easily. Typically, fresh snow has the density between  $50\text{-}100\text{ kg m}^{-3}$ . Compacted snow could be between  $300\text{-}500\text{ kg m}^{-3}$  and up to  $550\text{ kg m}^{-3}$ , if some of the snow was melted and refrozen. This could result in the increase of snow thermal conductivity between 1-2 orders of magnitude.

The lowest temperature recorded at the depth of 140 cm below the ground level at a 0.25 m distance from the thermosyphon was -2.7 °C in January 2019, however, no later record was available. Despite pump failure in December natural convection facilitated a consistent decrease of ground temperatures, however, the combined effects of pump-facilitated forced convection as well as reduction of snow cover around the thermosyphon allowed for the highest rate of ground heat transfer. An average temperature at the tube for all depths, for the winter season (mid Oct 2018-late Feb 2019) was -5.1 °C. At the end of August 2019 there was frozen ground present around thermosyphon/cone system at the depth of 70 cm below the ground surface ranging in radial distance from the edge of the cone from 55 to 90 cm. These results have been compared to previous approach proposed by Melnikov, et al., (1981) to calculate freezing radius for an Ideal Thermosyphon without Thermal Resistance which can be computed using expression (1):

$$R_0 \cong 0.9\sqrt[3]{dh^2} \quad (1),$$

where  $R_0$  is the limiting radius of ground freezing,  $d$  is the diameter of the thermosyphon, and  $h$  is the depth of the active layer. The predicted freezing radius ranges between 27.8 to 30.8 cm for  $h$  values of 60 and 70 cm. The average freezing radius recorded at the end of August 2019 was 70.1 cm, which is approximately 2.4 times greater than Melnikov`s approach.

During the following winter 2019/2020 the average temperature at the thermosyphon tube for all depths was -6.2 °C. However, due to the differences in the performance of individual components of the system (pump, battery) and research activity (timing of snow removal/compaction) in both years, it is impossible to conclusively determine the progression of performance of this system and the systematic rate of ground temperature changes. Nevertheless, these results suggest that it might be possible to re-establish permafrost within the talik using

ground cooling systems. To classify the ground as permafrost at Scotty Creek, it must remain at or below the temperature range between  $-0.14\text{ }^{\circ}\text{C}$  and  $-0.24\text{ }^{\circ}\text{C}$  (freezing point depression values) for at least two consecutive years. Considering the natural, site-specific permafrost aggregation dependent on presence of overlying dry peat, vegetation and south-facing aspect, it might be possible in the future to target locations that are likely to support natural permafrost aggradation. In the context of climate change, it might be possible to use thermosyphons to lower ground temperatures, for example in places that are undergoing desiccation, and remove them when natural conditions become sufficient to support permafrost.

#### **4.1.5. Insulated and non-insulated coaxial**

The performance of both insulated and non-insulated single-phase, passive, coaxial thermosyphons was assessed after a 6-week period after the installation at the beginning of February/2019 (Figure 10). The coaxial thermosyphons operate under the principle of natural advection with the guided fluid routing. In previously discussed designs the movement of operating fluids (isopropyl alcohol liquid and gaseous phase, and glycol-based coolant) is unrestrained, which can give rise to turbulent flow and decreased efficiency of heat transfer. The inner pipe in the coaxial design has a dual purpose, it separates the rising and sinking liquid generating lateral thermal gradients and facilitates routing of the moving fluid decreasing turbulent mixing.

Shortly after the installation the insulated coaxial achieved lower temperatures at 75 cm below the ground surface than the non-insulated coaxial (Figure 10a) due to more defined lateral gradients within the thermosyphon and more efficient heat transfer. The temperature profiles were converging for both designs during the 6-week period and in mid-March both designs

reached similar thermal profiles (Figure 10b). As the ground cools the thermal gradient between the inner and outer tubes in the insulated thermosyphon decreases and the rate of gravitational cycling approaches that of the non-insulated thermosyphon. The average temperature profiles for both thermosyphons for February and March (Figure 10c) also demonstrate the convergence of temperature trends although more studies are needed to investigate time-evolution of thermal processes for both designs.

## **4.2 Snow-shading cones**

### **4.2.1. Inter-site evaluation (between the groups)**

All cones were grouped according to the snow accumulation patterns. Cone1 and Cone5 appeared entirely covered by snow by February 2019, whereas Cone2 and Cone4 were only partially covered. There was a visible snow-free area around Cone4 (approximately 4 cm wide and 60 cm long) that allowed for air circulation and consequent temperature coupling under and outside of the cone. Similarly, there was a direct coupling of temperatures under and outside of Cone2. Thermal offset between the temperature of the air outside of and under the cone can be used as a snow insulation proxy (Figure 11a, b), with the high offset indicating ground insulation (Figure 11a). Average monthly temperatures under the cones illustrated inter-site characteristics (Figure 11c). For the period of August 2018/March 2019 Cone2 and Cone4 showed similar temperature profiles, whereas Cone1 and Cone5 displayed similar trends only after January. Between November and January, Cone1 and Cone5 exhibited similar temperature trends but of different magnitudes. These differences can likely be attributed to snow accumulation patterns around the cones and consequent variations in ground insulation.

The average temperature differences for Cones 1 (snow covered) and 2 (reduced snow), for the period of August/2018-March/2019 ranged between 1.2 °C at the ground surface and 0.7 °C at 80 cm below the ground surface. (These cones are used for comparison because of physiographic similarities of both locations). There was frozen ground present at the end of August 2019 at Cone 2 only however, the difference in temperatures is not only reflective of soil response to air temperature but as the moisture was moving towards the freezing front at Cone 2 at lower depths, some of it froze and latent heat released increased the temperatures of the soil profile.

#### **4.2.2 Intra-site evaluation (within each group)**

Temperature profiles under cones 1 and 5 exhibited similar trends after the snow removal at the beginning of February (Figure 12a, b). Prior to February 2019 the temperature profile for Cone 1 appeared stable whereas for Cone 5 it appeared to fluctuate which could be attributed to early snow accumulation patterns. Cone 5 was situated in a relatively open area and visual images from the wildlife camera provided qualitative evidence that snow accumulation patterns at both cones differed significantly. Cone 5 was subjected to frequent snow drifts and snow accumulation was less substantial as compared to more sheltered areas, such as Cone 1, which reduced the thermal insulation of the snowpack. Although location of Cone 1 was not equipped with a wildlife camera, locations of cones 1 and 3 were comparable in terms of vegetation and microtopographic shelter. Cone 3 was equipped with wildlife camera and therefore after comparing visual images for cones 3 and 5 the inference can be made that Cone 1 had higher depth of accumulated snow around it than Cone 5.

It was estimated that snow depth at Cone5 remained below 50 cm for most of the season, whereas at Cone3(West site) it was estimated between 80-100 cm at the end of December. Cones 2 and 4 exhibited similar temperature profiles during first season (Figure 12c, d). Thermal offset between air temperatures under and outside of the cones was low (Figure 11a), it was evaluated by considering the annual air temperature ranges under and outside of the cones and expressing the difference between them as a percentage of the outside range. The average difference between both temperature ranges was 3.4% for Cone2 and 3.2 % for Cone4. These results suggest a very good air exchange under the cones. At the end of August 2019 there was a 15 cm thick frozen layer around both cones at a depth between 60-75 cm below the ground surface. The radial distance of the frozen ground was on average approximately 50 cm from the edge of the cone. There was no frozen layer around cones 1 and 5.

During the 2018/2019 winter season (Oct/2018-Feb/2019) the average temperatures for Cone4 at 5, 25, and 50 cm were -2.1 °C, -0.5 °C and -0.004 °C respectively. In the following winter 2019/2020 those temperatures further decreased to -3.6 °C, -2.1 °C and -0.32 respectively (Figure 12e). Similar trend was noted for Cone2 with temperatures at 5 cm decreasing from -2.7 °C to -5.1 °C, at 25 cm from -0.9 °C to -2.3 °C and at 50 cm from 0.01 °C to -0.5 °C. The differences in magnitudes between the cones are most likely attributed to different snow accumulation patterns. Both cones were installed in sheltered areas along the seismic line adjacent to peat plateaus however, Cone4 was installed under a mature tree (*Picea mariana*), where expected snow interception and redistribution are likely to affect accumulation patterns.

### **4.2.3 Evaluation of 1-D heat conduction model for calculating depth of freeze at Cone1 and Cone2**

Depth of freeze estimated by 1-D heat conduction model (Braverman, Personal Communications) for cones 1 and 2 was 47 cm and 63 cm, respectively (Figure 13a, b). It was impossible to confirm the exact predicted freeze depth due to a lack of instrumentation at those depths and  $\pm 0.2$  °C margin of instrumental error, however, these results are consistent with the in-situ temperature measurements. At the end of August 2019 there was a 15 cm thick frozen layer around Cone2 at the depth between 60-75 cm below the ground surface, which is consistent with the predicted depth of freeze. The radial distance of the frozen ground was on average approximately 50 cm from the edge of the cone.

### **4.2.4 Ground insulation under Cone5 and under direct snowpack**

An observed difference between the ground temperatures directly under the snowpack (B) and under a snow-covered Cone5 (A), (Figure 14a) suggests increased insulation under the snow-covered cone (Figure 14b). As the cone became entirely covered by snow (including the bottom part between the base and the ground, and the top opening) air exchange was prevented. The heat flux transmitted from the ground warmed the air above the surface which remained trapped under the cone for the duration of the snow-insulated period. Considering low thermal diffusivity of air and snow insulation of the cone, the dissipation of heat from under the cone was impeded and the snow-covered cone insulated the ground more than the snowpack itself. Average temperatures at the ground surface under the snow-covered cone were 1.8 °C warmer than under the snow outside of the cone, with the maximum difference of 3.0 °C. Implications of these findings can inform future snow-shading designs. Distinct annual heat transfer processes

were observed under the cone during the snow-free period, indicated as intervals I, II, III, IV. (Figure 14 b). During the initial period (I) from the end of August 2018 until mid November 2018 before stable snowcover was established, the ground temperature under the cone appeared lower and less fluctuating than outside of the cone. The cone was shielding the ground from direct solar radiation which is the most likely reason for this temperature difference. During phase (II) from the end of November 2018 till the end of December/2018 both temperatures converged. At that time the cone became gradually covered by snow, which allowed for stabilization of ground temperatures outside of the cone by inhibiting the ground heat fluxes. During the snow-insulated period there was a characteristic thermal offset between the temperatures. Ground temperatures under the cone increased as the ground heat fluxes warmed the air trapped under the cone and became stable when the heat fluxes diminished. Snowcover was removed from around the cone at the beginning of phase (III) and temperatures converged between mid February 2019 and mid March 2019. During phase (IV) temperatures outside the cone started increasing due to unusually warm air temperatures during March 2019 and the following seasonal warming, whereas ground level under the cone experienced an extended zero-degree curtain period most likely due to shading preventing direct solar radiation. Exploring these processes is recommended to better understand the thermal characteristics of a snow shading cone under a range of climatic conditions.

#### **4.2.5. Preliminary snow insulation assessment**

The interpretation of snowpack evolution can be achieved by evaluation of temperatures recorded by vertical array of sensors (Danby and Hik, 2007; Lewkowicz, 2008). At Cone5 seasonal convergence of air temperatures and temperatures at 50 cm above the ground suggest

that snow cover at that location was less than 50 cm in depth. There were no wildlife camera records available to confirm this after the beginning of January due to battery failure. Short periods of decoupling between ambient air temperatures and temperatures at 50 cm above the ground level were likely due to snow-drifting events and/or possible instrumental differences between temperature sensors outside of Cone3 and at the MET station. However, thermal profiles at 10 and 30 cm above the ground surface exhibited recurrent thermal offsets which indicates presence of snow (Figure 15).

During the month of January, the thermal offset between the air temperature and at 30 cm above the ground level was the greatest. At that time temperature at 10 cm below ground level appears most stable despite air temperatures fluctuations ( $STDEV.S=0.29$ ), which suggests that during this period snow insulation was the strongest.

### **4.3 Recommendations**

Although thermosyphon technology has been used to suit a range of applications for over 60 years and its purpose is well acknowledged, the alarming rate of climate change in the North emphasizes the importance of new mitigation and adaptation strategies. The increasing geographic accessibility that accompanies warming climate enables expanding resource exploration and development of the North, simultaneously challenging pre-existing infrastructure. Considering the increasing demand of ground thermal stabilization technologies, the novel ground cooling systems must integrate performance and deployment efficiency, maintenance accessibility and cost considerations.

Our evaluation of seven freezing systems emphasizes the importance of case-based approach with careful consideration of individual application goals and environmental

conditions. In the case of the single-phase, active thermosyphon conjoined with a snow shading cone, the soil profile with direct shading was subjected to a large vertical temperature gradient formed in the absence of snow. This suggests that at the beginning of the cold season there was a significant vertical upward energy flux within the seasonally frozen layer of approximately 60 cm below the ground surface. We recommend detailed investigation, both laboratory and in situ to further explore the thermal gradients resulting from snow removal and thermosyphon operation.

We propose that the heat transfer and subsequent density changes affect only the volume of the coolant adjacent to the thermosyphon wall and we recommend further studies of the extent of those changes.

The stand-alone snow shading cone can shield the ground from direct solar radiation hindering ice thaw in early spring and evaporation and desiccation in the summer. It could potentially warm up on a clear, sunny day and when surrounded by thick vegetation, create a localized warmer area which would be detrimental for permafrost stability. Further investigation of the processes governing heat fluxes above the ground under the cone, such as turbulent movement of air and heat exchanges between the cone material (e.g. steel, aluminum, etc.) and the atmosphere is recommended to inform future designs. We have demonstrated that snow accumulation patterns around the cones have significant effect on ground cooling however, structural limitations of the design prevent more effective snow exclusion and require future development and improvement. We recommend an auxiliary system that could aid in snow elimination in future designs. Depending on site specific conditions these systems could include

snow fencing around the cones, overhanging tarp coverings and dark cone screens. Larger cone designs are also a possibility however, logistic limitations must be considered.

The coaxial designs are showing promising cooling capacity with no energy dependence and minimal servicing needs making them an economically viable option for ground temperature control and permafrost stabilization. Future research is needed to quantitatively compare both designs and further examine their effectiveness in the changing peatland environment. Snow removal is also recommended to further increase their efficacy.

## **5. Conclusions**

Determining the thermal regime of the soil profile is crucial in interpreting ecosystem responses to climate change and it is also very important in many scientific and engineering applications. This study has shown that both passive and active ground freezing systems can be utilized to control ground temperatures in highly saturated peat environments. We have evaluated seven freezing systems. Single-phase active thermosyphon design conjoined with the snow shading cone demonstrated highest ground cooling efficiency however, coaxial designs appear to be very efficient and have no-energy dependency. We have shown that snow plays an essential part in an annual ground thermal regime. Ground temperatures with snowpack present were on average by 1°C warmer than those in snow-free areas, however, when interpreting those temperature differences processes other than snowpack must be considered as well. The intra-site variability for both groups of cones within seasonally frozen layer, between 0-60 cm, can be attributed to snow accumulation patterns. Below 60 cm that variability is most likely due to the presence of unfrozen moisture content. These findings confirm that snow influences ground thermal responses directly by insulation, however other processes can offset this influence e.g.

release of latent heat during freezing. Ground temperatures must be therefore interpreted with that in mind.

We emphasize the importance of identifying localized geophysical and environmental conditions as the basis for determining the most suitable cooling system for mitigation and control of ground thermal profiles. We recommend developing a thorough understanding of goals and expectations of enhanced ground cooling technology on an individual, case-based approach for most efficient thermosyphon design selection. This investigation is projected to support the development of low cost, readily-deployable ground cooling devices that may serve to mitigate permafrost thaw and improve the adaptability of engineering designs to a wide range of changing environmental conditions and aid in controlling ground temperatures in non-permafrost regions that experience periodic freeze and thaw cycles.

## 6. Appendix A-Figures

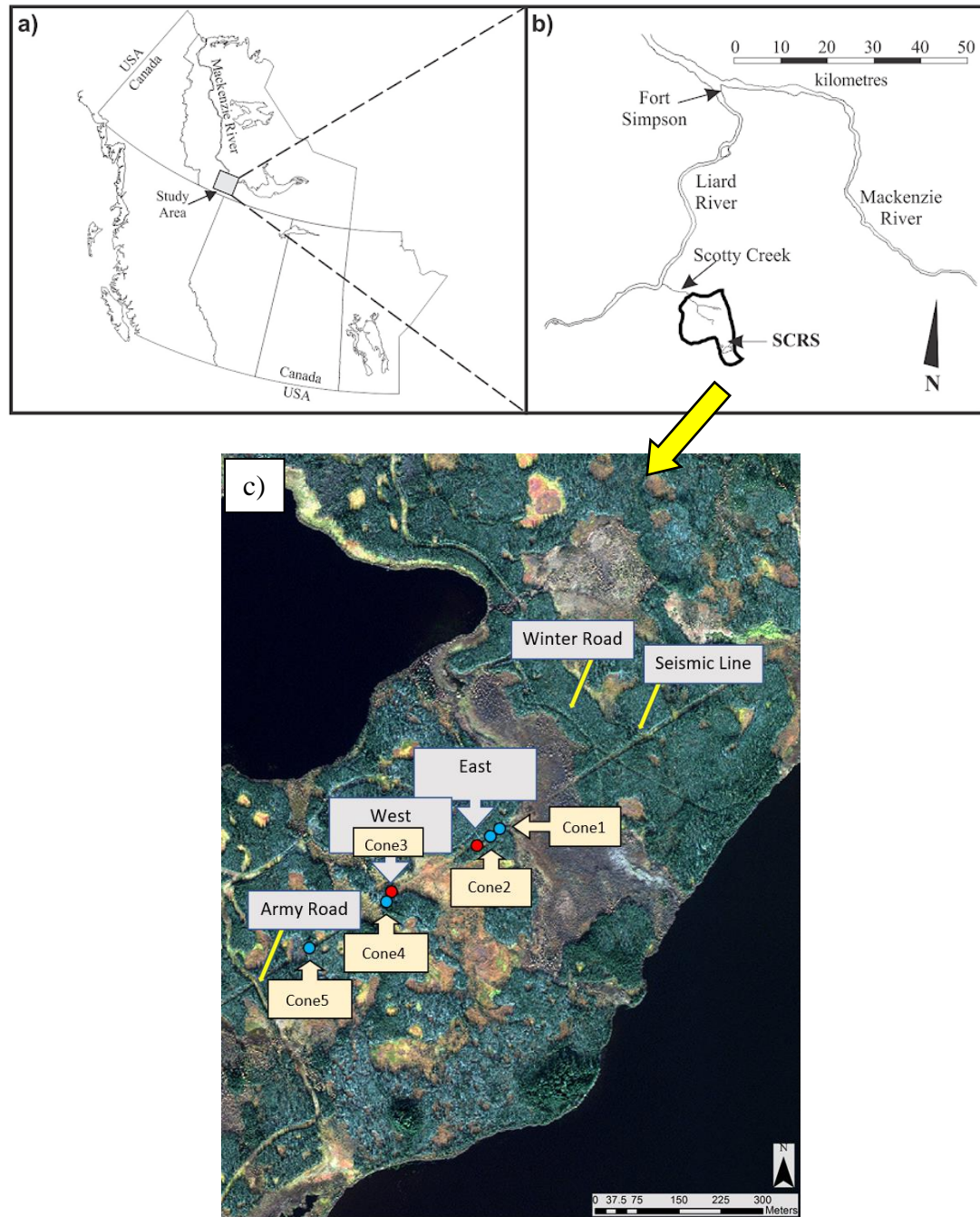
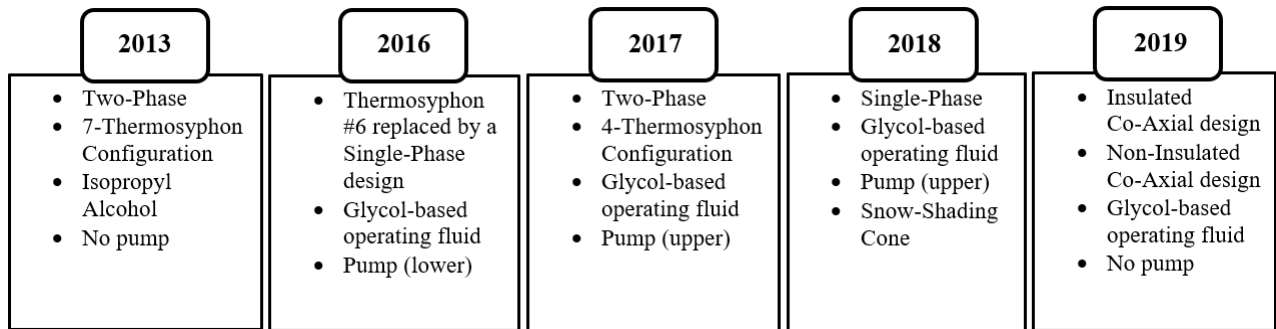


**Figure 1.** (a) Map of the study area within Canada (Image adapted from Connon et al., 2018), (b) Scotty Creek region. Basin boundaries represent the area of the basin gauged by the Water Survey of Canada, (c) Study Site location within the Scotty Creek Research Station

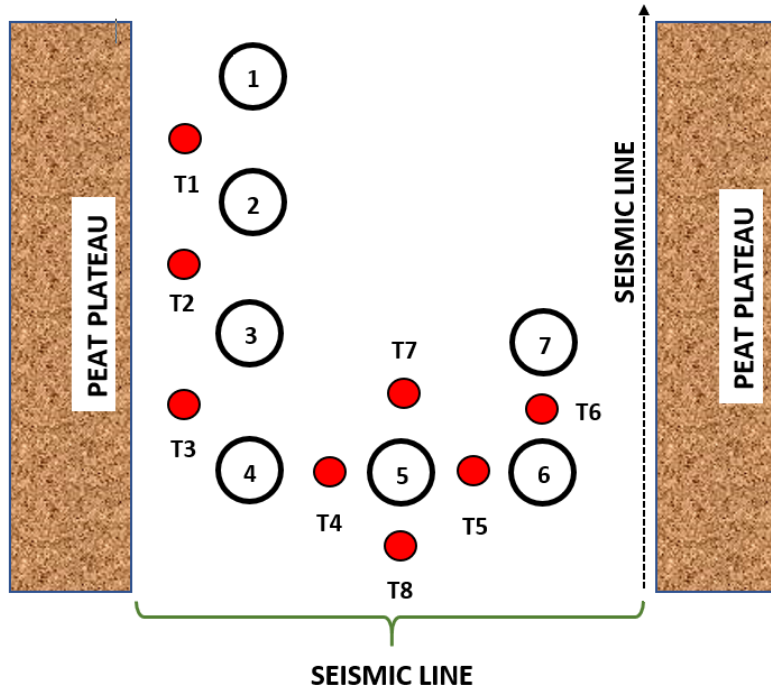


a)

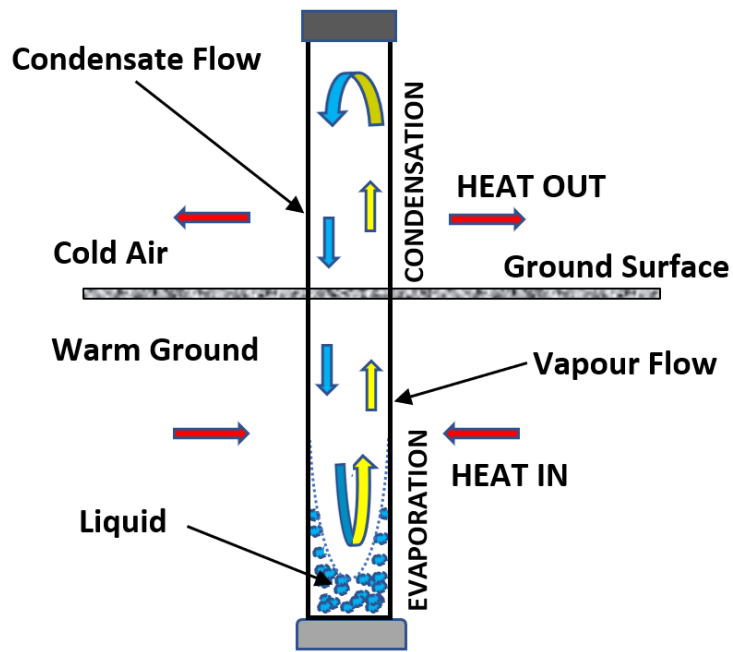
Physical properties	Types of Operating Substance	Principles of Operation
<ul style="list-style-type: none"> <li>• Thermal Diffusion</li> <li>• Phase Change</li> <li>• Advection</li> <li>• Radiation</li> </ul>	<ul style="list-style-type: none"> <li>• Liquid CO<sub>2</sub></li> <li>• Ammonia</li> <li>• Kerosene</li> </ul>	<ul style="list-style-type: none"> <li>• Passive</li> <li>• Active</li> </ul>

b)

**Figure 2.** (a) Summary of Thermosyphon Research and Design Evolution at Scotty Creek, (b) Considerations for Thermosyphon Design



a)



b)

**Figure 3.** (a) Aerial view of two-phase, passive7, (b) Two-phase, passive thermosyphon

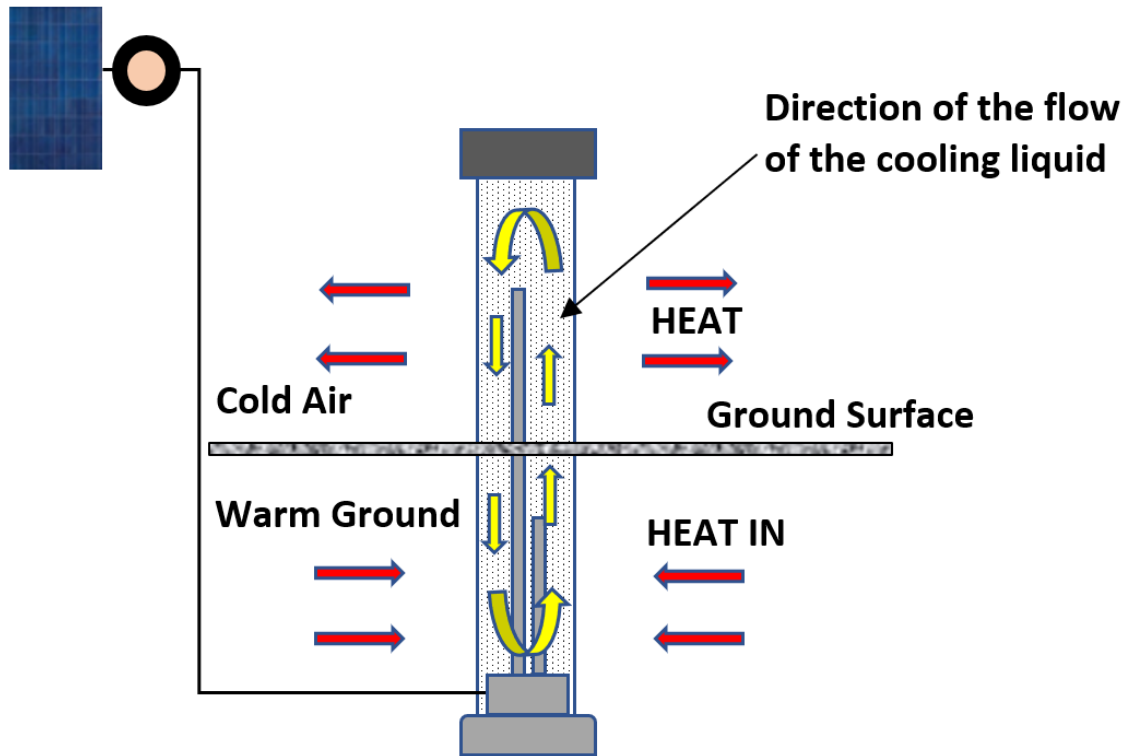
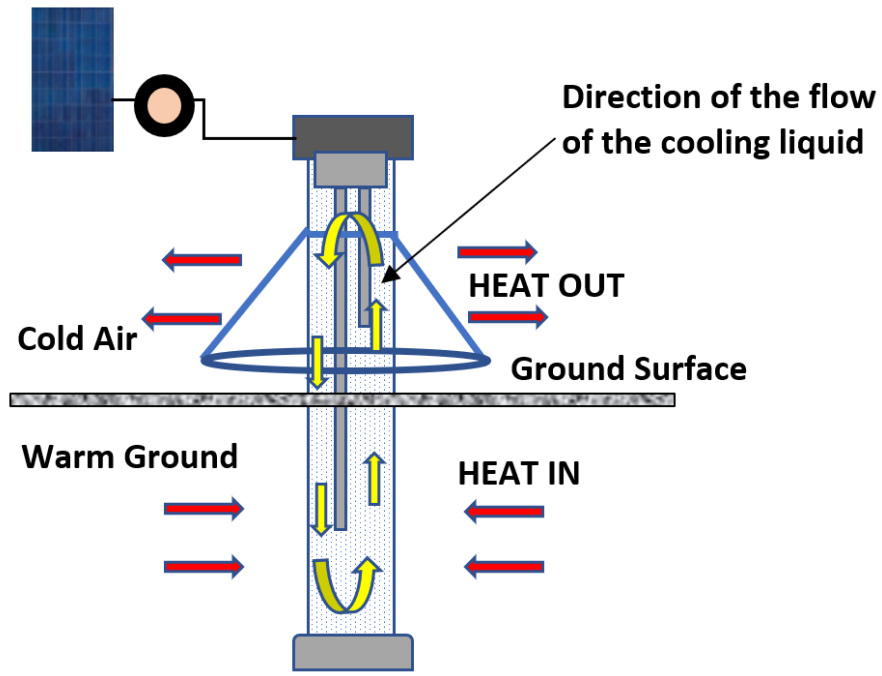
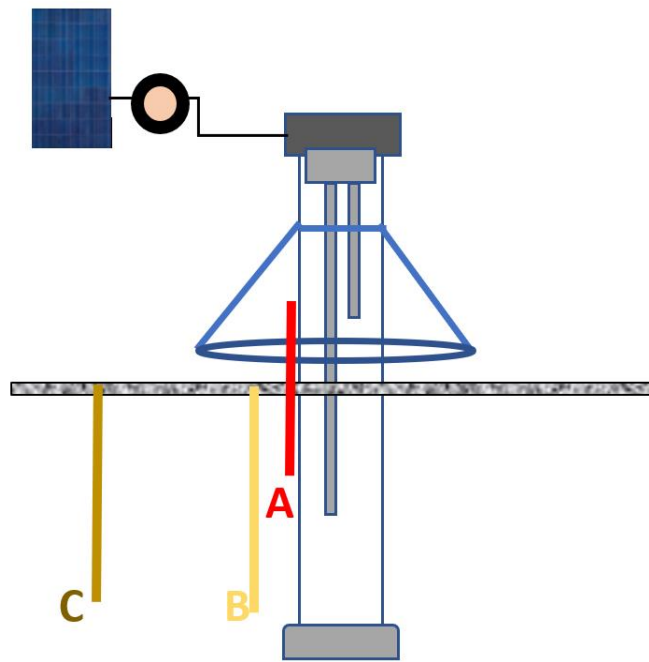


**Figure 4.** Single-phase, active thermosyphon with a lower pump

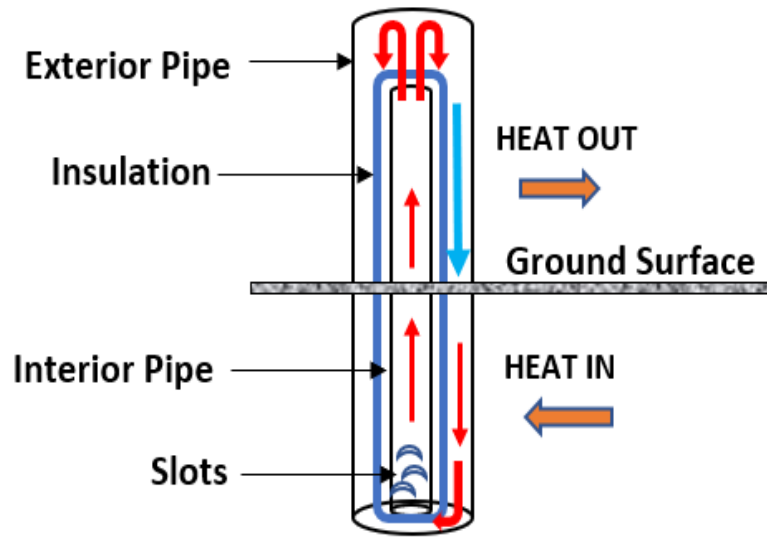


(a)

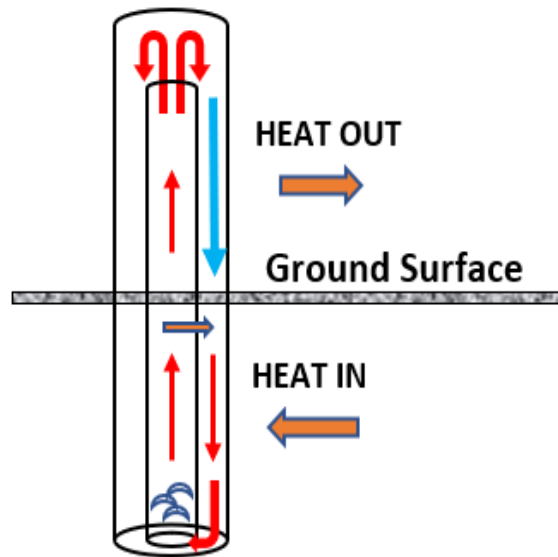


(b)

**Figure 5.** (a) Single-phase, active thermosyphon (upper pump), conjoined with the snow shading cone, (b) Thermistor sets at single-phase, active thermosyphon with a cone



(a)



(b)

**Figure 6.** Single-phase, passive, coaxial thermosyphon (a) Insulated, (b) Non-Insulated



(a)



(b)

**Figure 7.** (a) Snow-shading cone, (b) Thermosyphon conjoined with a snow-shading cone

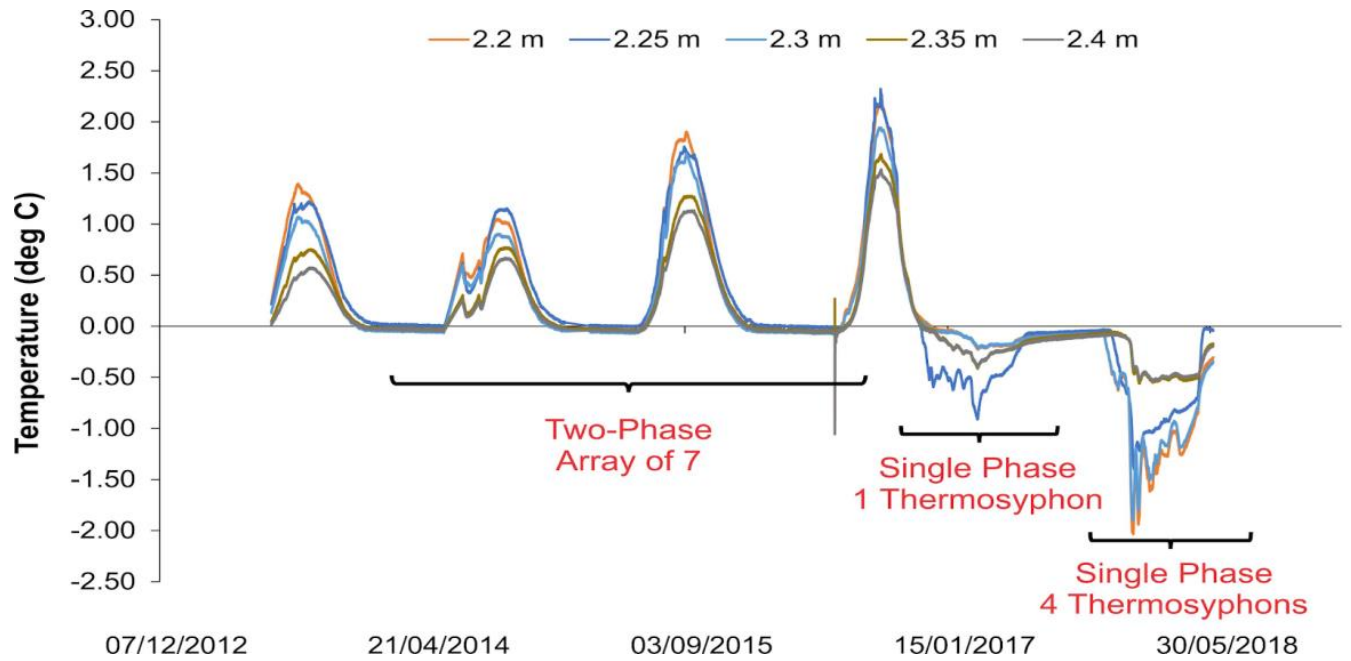
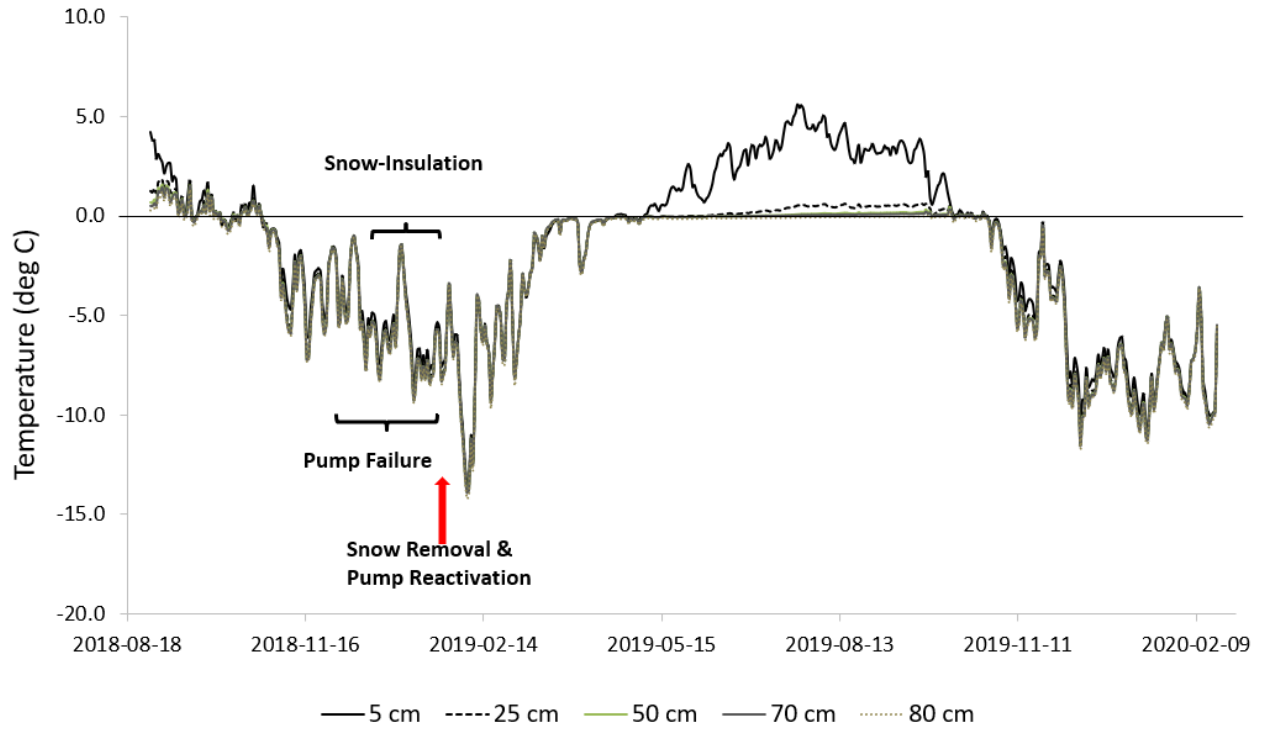
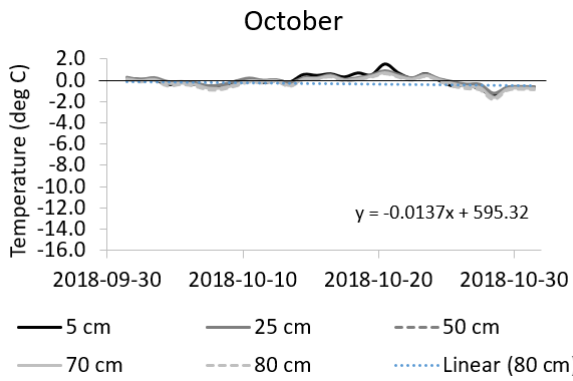


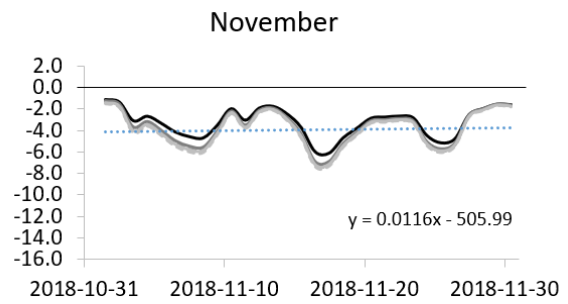
**Figure 8.** Temperature profiles at 0.25 m distance from the wall of thermosyphon 6 for two-phase, passive, 7-thermosyphon; single-phase, active thermosyphon and single-phase, active 4-thermosyphon configuration for the period of 2013-2018



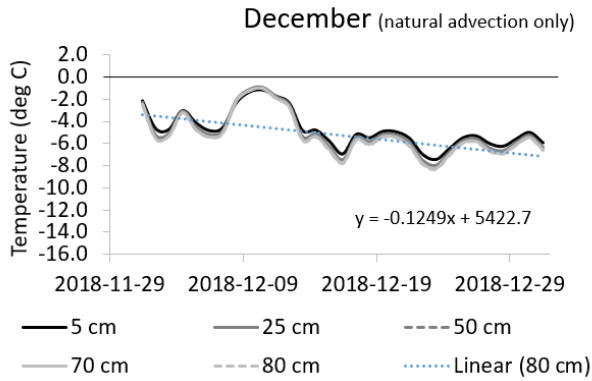
(a)



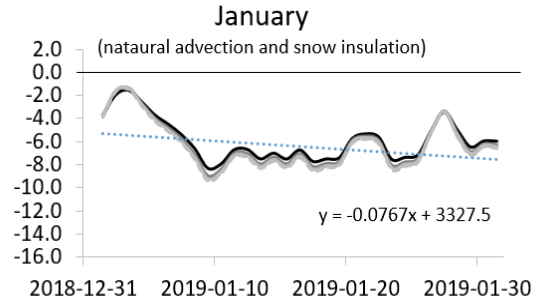
(b)



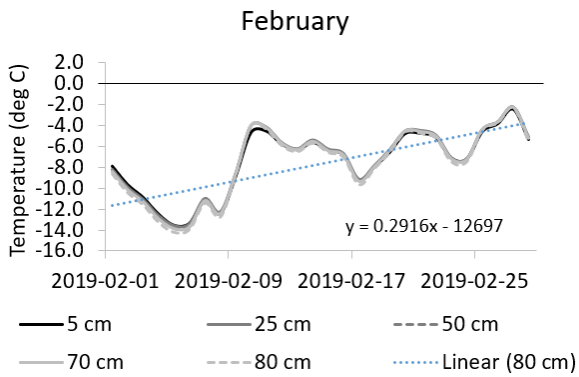
(c)



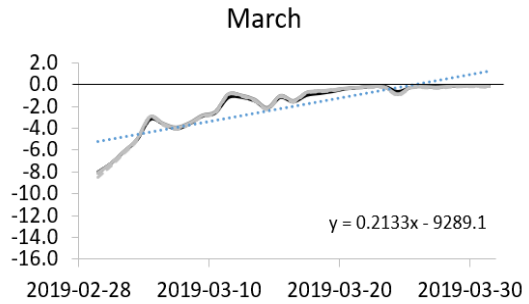
(d)



(e)



(f)



(g)

**Figure 9.** Temperature profiles at the thermosyphon tube for the single-phase, active thermosyphon with a cone, for the period of (a) Aug 2018-Feb 2020, (b) October 2018, (c) November 2018, (d) December 2018, (e) January 2019, (f) February 2019, (g) March 2019

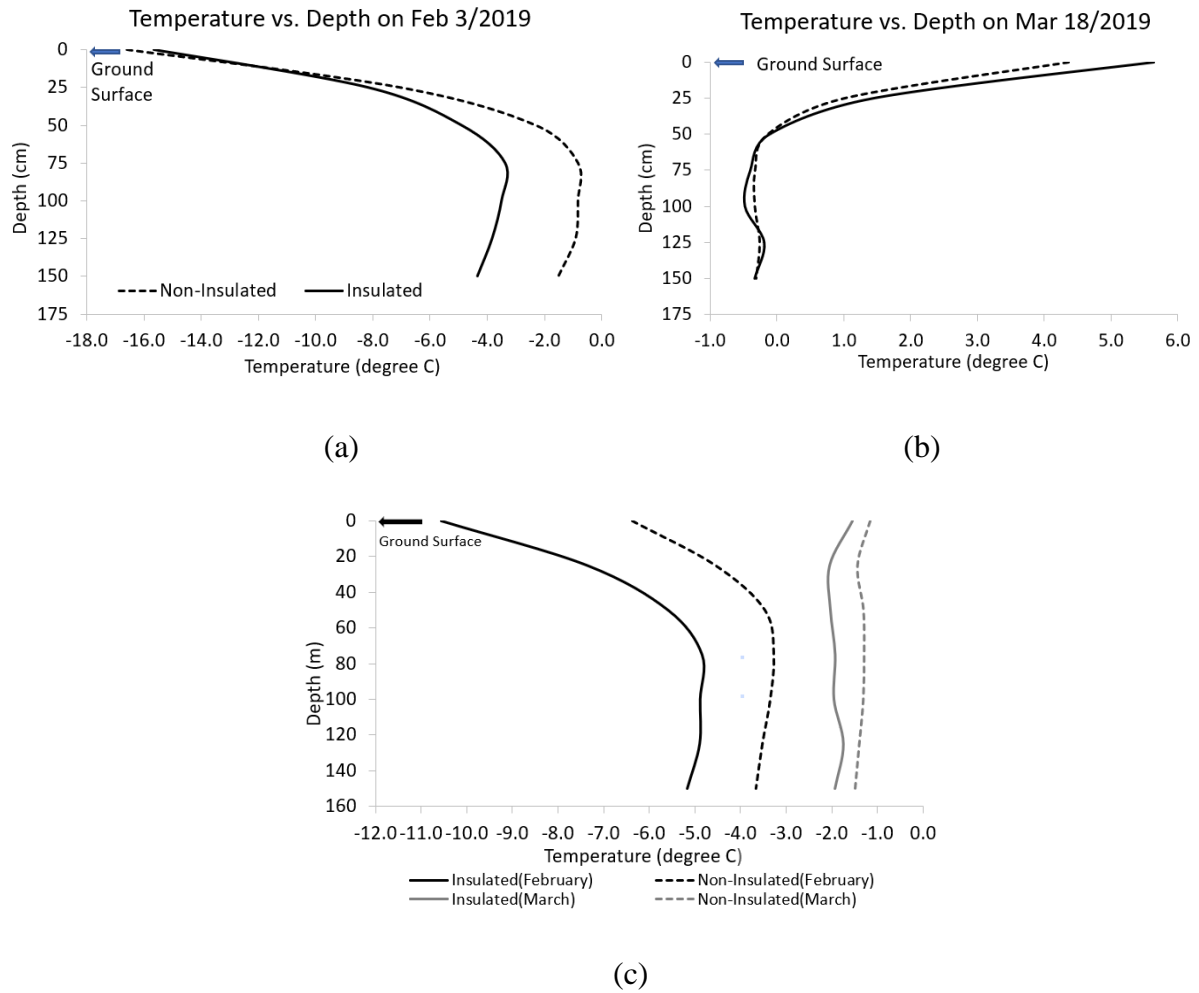
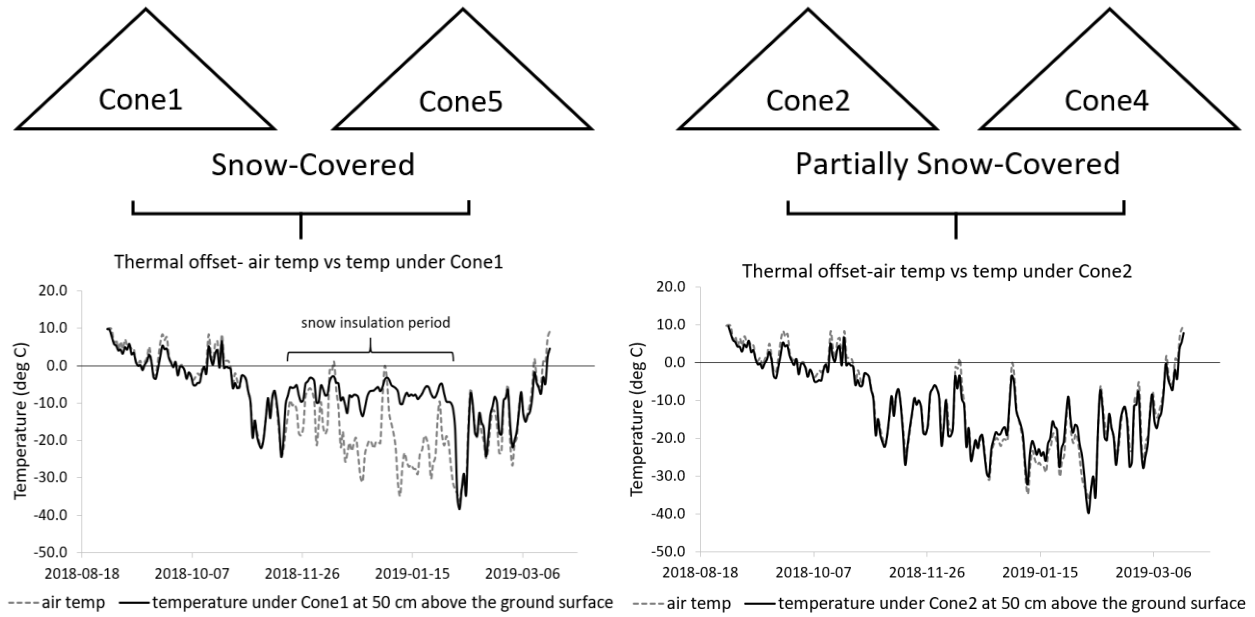
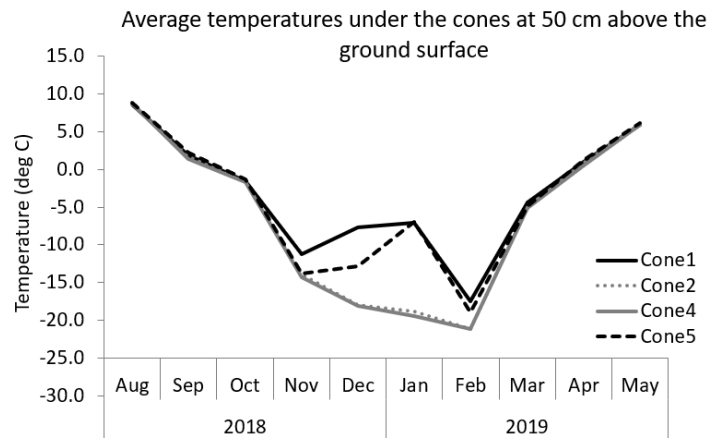


**Figure 10.** Ground temperatures for Insulated and Non-Insulated Coaxials on (a) Feb3/2019, (b) Mar 18/2019 and (c) Average monthly temperatures for February and March



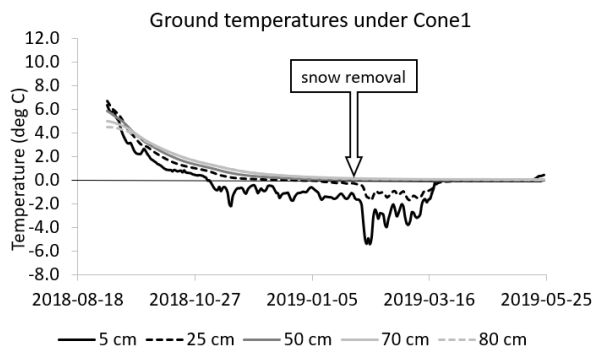
(a)

(b)

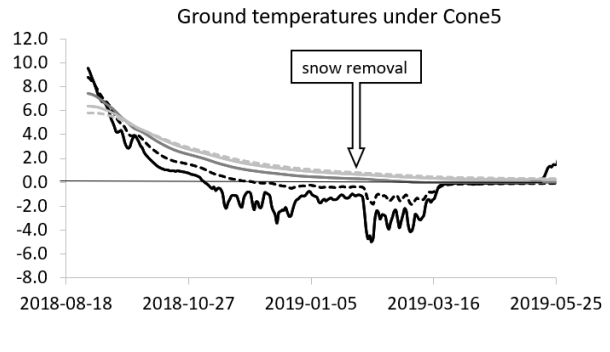


(c)

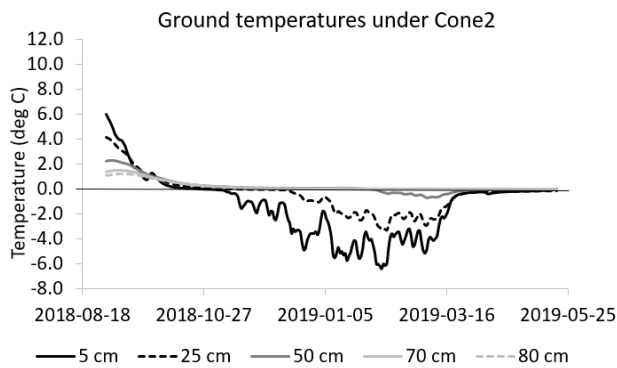
**Figure 11.** Temperature profiles for (a) snow-covered Cone1, (b) partially snow-covered Cone4, and (c) average monthly temperatures under cones 1, 2, 4, 5 recorded 50 cm above the ground surface



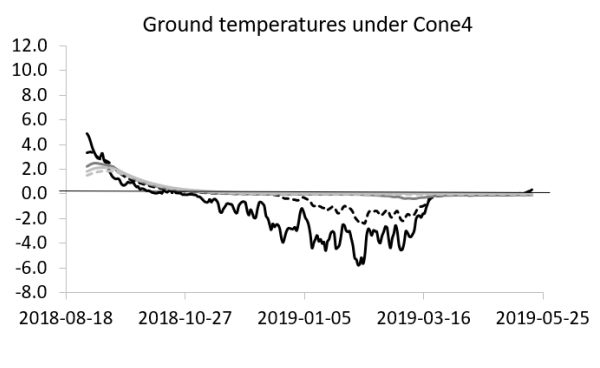
(a)



(b)

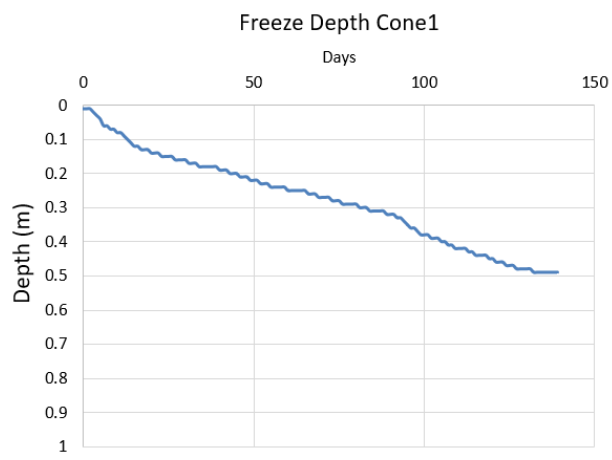


(c)

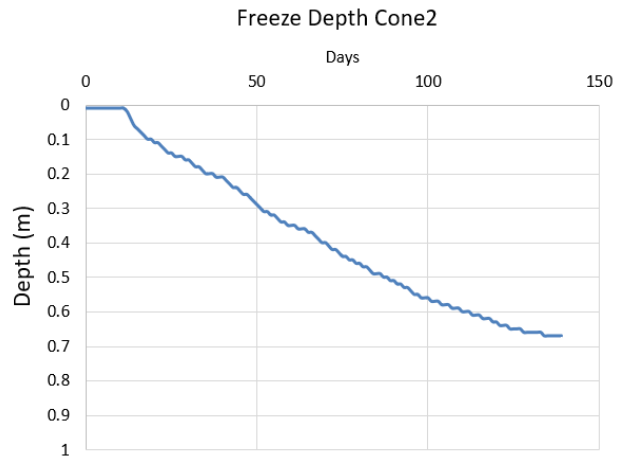


(d)

**Figure 12.** Ground temperature profiles for (a) Cone1, (b) Cone5, (c) Cone2, (d) Cone4,

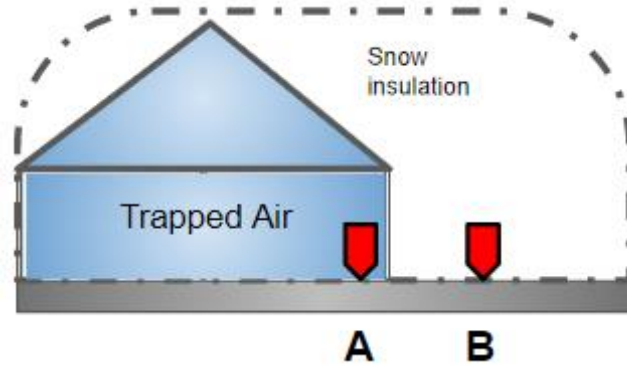


(a)

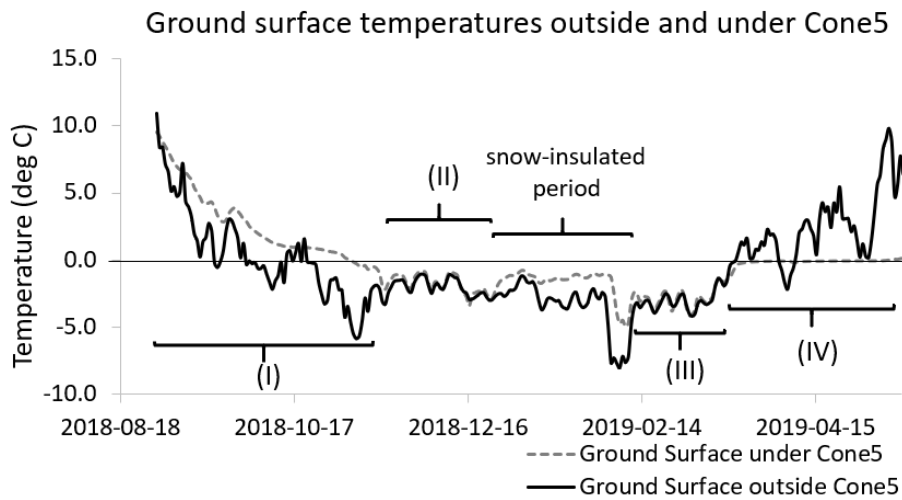


(b)

**Figure 13.** Simulated Freeze Depth for (a) Cone1 and (b) Cone2



(a)



(b)

**Figure 14.** (a) Ground insulation diagram; ground level directly under the snow (B) and under the snow-covered cone (A), (b) Temperature profiles at (A) and (B)

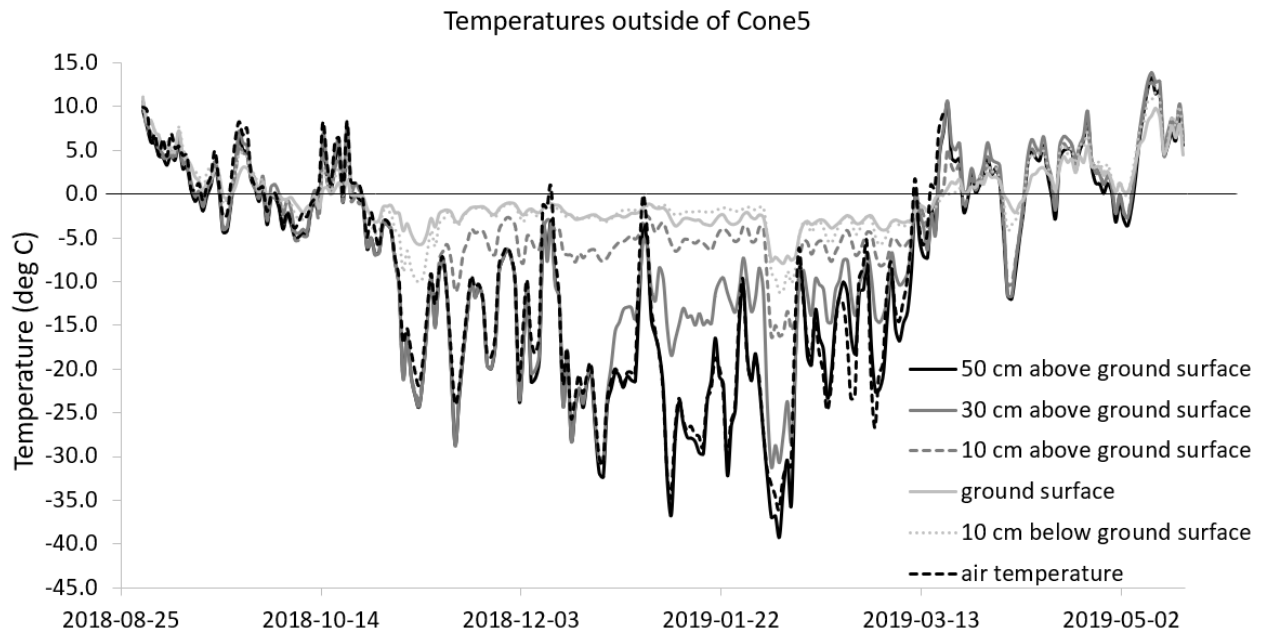


**Figure 15.** Temperature profiles above the ground surface outside of Cone

## Chapter 3: Conclusion

Northern ecosystems and their communities are facing increasing environmental challenges and concurrent socioeconomic changes. Significant warming in the recent decades has increased the accessibility of natural resources and economic feasibility of their development. The growing need for efficient climate-change mitigation strategies to support new and existing infrastructure has become a pivotal subject in future agendas of northern development. New strategies must address changing dynamics of permafrost configuration. This research aims to contribute to the understanding of cooling systems in peat-based environments. The main objective of thermosyphon design evolution is to develop a system that not only delivers the best cooling outcomes as expressed by the rate, magnitude and spatial extent of cooling, but also considers annual site access, service availability and robustness of energy sources (if needed).

This study evaluated the performance of seven ground cooling systems installed at Scotty Creek Research Station, NT, between 2013-2019. These systems were: (1) **two-phase, passive**, (2) **single-phase, active**, (3) **single-phase, active**, (4) **single-phase, active with a cone**, (5) **4 individual snow cones**, (6) **non-insulated coaxial** and (7) **insulated coaxial**.

We have shown that the single-phase designs are substantially more efficient in peat-based substrates than two-phase designs. Two-phase systems are contingent on latent heat fluxes during phase changes and are reliant on liquid-to-gas ratios, whereas single-phase systems utilize the size of the system (larger amount of operating fluid) for energy transfer. However, it has been suggested (Egorov, Personal Communications) that temperature changes occur only within the thin film of operating fluid adjacent to the thermosyphon wall. Although enhanced circulation

increases the rate of heat transfer, thermal gradients are the limiting factors of overall efficiency. Coaxial designs focus on increasing the internal temperature gradients and improving the effectiveness of liquid routing, consequently increasing heat transfer efficiency. After a limited period of study these designs have demonstrated a noteworthy ground cooling capacity although more long-term studies are needed to quantify their efficiency. Snow exclusion in conjunction with thermosyphons creates vertical temperature gradients and increases heat transfer efficiency as evidenced by the sudden drop in ground temperatures upon snow removal in early February 2019.

More extensive studies in a controlled environment are recommended to quantify cooling efficiency of each system. We recommend determining a cooling coefficient of each system which would express cooling efficiency as a function of maximum achievable heat transfer. We emphasize the importance of thorough understanding of individual projects as well as operational limitations prior to selection of the most suitable system.

We also would like to address the possibility of a cooling system (individual snow shading cone) to exhibit analogous properties to a natural environmental component (tree), by considering a question: Can a snow shading cone imitate a tree with respect to its effect on the ground thermal regime?

Plant communities in permafrost environments, including trees, shrubs and mosses, play a vital role in controlling the temperature of soil, and therefore the presence of permafrost. Plants shade the soil from the warmth of sunlight, and their roots extract water leading to drier soils which are better insulators.

The potential similarity between a tree and a snow shading cone with respect to its effect on ground thermal regime must be determined in the context of their individual impacts on the energy balance at the soil surface, immediate atmospheric boundary layer and the soil profile (active layer and below). Considering the complexity of the variables affecting the energy balance those impacts vary in time and space. The most obvious physical similarity between a tree stand and a snow shading cone is its capacity to shade the ground from solar radiation and shelter it from snow. The most important source of energy is incident solar radiation (shortwave). It can be reflected, absorbed or transmitted according to the physical properties of the medium which constitute their albedo. Tree trunk (complex carbohydrates) has an albedo of 0.09, whereas snow shading cone is made of galvanized stainless steel and has an albedo of 0.35, reflecting substantially more shortwave radiation. However, albedo varies in time and space and its value depends primarily on the amount of diffuse radiation (clear vs cloudy day), an angle of incidence (season/aspect/shading), and to a lesser extent physical property of an object. Another important parameter to consider is the emissivity, which depends on the temperature of an object and the emissivity coefficient. The tree stand has a much higher emissivity (IR spectrum) (0.97) (Birbeback and Birbebak, 1964) than the galvanized steel (new GSS- 0.28) (metal Index).

Tree emissivity varies with species (Leuzinger et al, 2010), however conifers (predominant species at Scotty Creek, NT) have small boundary layer resistances (Martin et al. 1999; Jarvis et al. 1976), leading to a rapid exchange of sensible heat and a large heat transfer, which results in a close coupling between needle and air temperatures (Jarvis et al. 1976), and it has frequently been assumed that conifer needle temperatures rarely differ from air temperature by more than 1°C (Angell and Miller 1994; Jarvis et al. 1976; Kaufmann 1984). Since the insolation (exposure to solar radiation) of both the tree stand and the snow shading cone affects

the amount of energy absorbed and their consequent temperature, it influences their emissivity of IR radiation. Due to their varying properties, the response to climatic variables of the tree stand and the snow shading cone can vary substantially. However, those responses do not always affect the ground thermal regime. For example, in certain circumstances even on a sunny day, high emissivity of a tree can be counteracted by high wind speed (larger than 2 m/s) or high humidity, since water vapor is the single most important absorber in the IR band (Petty 2006). Conversely, depending on location and the insolation, the tree stand can be much warmer than the effective brightness temperature of the sky (Spittlehouse et al., 2004).

It can be assumed that on a cloudy day in late summer/early fall when the angle of incident radiation is relatively high and wind speed exceeds 2 m/s, a coniferous tree located on the north facing side maintains approximate temperature of the air. The same can be assumed for a snow shading cone if experiencing the same climatic conditions. It can be further assumed that although the tree and the cone have different emissivities, their input into surface energy balance might be comparable in such circumstances. However, they cannot be comparatively assessed below the ground surface due to complex root system of a tree and because a snow cone does not participate in mass exchange through the extraction of moisture.

It can be concluded that the similarities between the snow shading cone and a coniferous tree stand with regards to their effects on the ground surface energy balance can be established for a restricted set of climatic conditions and would require a detailed field investigation.

A similar conclusion can be reached with regards to comparison of a tree stand and a deactivated thermosyphon.

## Chapter 4: References

- Angell RF, Miller RF. 1994. Simulation of leaf conductance and transpiration in *Juniperus occidentalis*. *Science* **40**: 5–17.
- Akerman HJ, Johansson M. 2008. Thawing permafrost and thicker active layers in sub-arctic Sweden. *Permafrost and Periglacial Processes* **19**(3): 279-292.
- Baltzer J, Veness T, Chasmer L, Sniderhan A, Quinton W. 2014. Forests on thawing permafrost: Fragmentation, edge effects, and net forest loss. *Global Change Biology* **20**(3): 824- 834.
- Beck I, Ludwig R, Bernier M, Lévesque E, Boike J. 2015. Assessing permafrost degradation and land cover changes (1986–2009) using remote sensing data over Umiujaq, sub-arctic Québec. *Permafrost and Periglacial Processes* **26**(2): 129-141.
- Beilman DW, Vitt DH, Halsey LA. 2001. Localized permafrost peatlands in western Canada: definition, distributions, and degradation. *Arctic, Antarctic and Alpine Research* **33**(1): 70–77.
- Birbeback R, Birbebak R. 1964. Solar radiation characteristics of tree leaves. *Ecology* **45**: 646-649.
- Bokhorst S, Pedersen SH, Brucker L, Anisimov O, Bjerke JW, Brown RD, Ehrich D. 2016. Changing Arctic snow cover: A review of recent developments and assessment of future needs for observations, modelling, and impacts. *A Journal of the Human Environment* **45**(5): 516-537.
- Braverman M, Quinton WL. 2016. Hydrological impacts of seismic lines in the wetland-dominated zone of thawing, discontinuous permafrost, Northwest Territories, Canada. *Hydrological Processes* **30**(15), 2617–2627.
- Braverman M, Quinton WL. 2017. An experimental study of permafrost restoration under seismic line in wetland-dominated zone of discontinuous permafrost, Northwest Territories, Canada, in: GEO Ottawa 2017, 1–4 October 2017, Ottawa, Canada, 2017.
- Bridgham SD, Johnston CA, Pastor J, Updegraff K. 1995. Potential Feedbacks of Northern Wetlands on Climate Change. *BioScience* **45**(4): 262-274.
- Burgess MM, Smith SL, Brown J, Romanovsky V, Hinkel K. 2000. Global Terrestrial Network for Permafrost (GTNet-P): Permafrost Monitoring Contributing to Global Climate Observations. Geological Survey of Canada, Current Research 2000-E14; 8 pp.
- Camill P. 1999. Patterns of boreal permafrost peatland vegetation across environmental gradients sensitive to climate warming. *Canadian Journal of Botany* **77**(5): 721–733.
- Carpino OA, Berg AA, Quinton WL, Adams JR. 2018. Climate change and permafrost-thaw induced boreal forest loss in northwestern Canada. *Environmental Research Letters* **13**(8):
- Chasmer L, Hopkinson C, Veness C, Quinton WL, Baltzer J. 2014. A decision-tree classification for low-lying complex land cover types within the zone of discontinuous permafrost. *Remote Sensing of Environment* **143**: 73-84.

- Chasmer L, Hopkinson C. 2017. Threshold loss of discontinuous permafrost and landscape evolution. *Global Change Biology* **23**(7): 2672–2686.
- Cline DW. 1997. Effect of seasonality of snow accumulation and melt on snow surface energy exchanges at a continental alpine site. *Journal of Applied Meteorology* **36**(1): 32-51.
- Cohen J. 1994. Snow cover and climate. *Weather* **49**(5): 150-156.
- Connon RF, Quinton WL, Craig JR, Hayashi M. 2014. Changing hydrologic connectivity due to permafrost thaw in the lower Liard River valley, NWT, Canada. *Hydrological Processes* **28**(14): 4163–4178.
- Connon R, Quinton WL, Craig JR, Hanisch J, Sonnentag O. 2015. The hydrology of interconnected bog complexes in discontinuous permafrost terrain. *Hydrological Processes* **29**(18): 3831-3847.
- Danby RK, Hik DS. 2007. Responses of white spruce (*Picea glauca*) to experimental warming at subarctic alpine treeline. *Global Change Biology* **13**(2): 437-451.
- Davidson DJ, Williamson T, Parkins JR. 2003. Understanding Climate change risks and vulnerability in northern forest-based communities. *Canadian Journal of Forest Research* **33**(11): 2252-2261.
- Derksen C, Brown R. 2012. Spring snow cover extent reductions in the 2008-2012 period exceeding climate model projections. *Geophysical Research Letters* **39**(19).
- Dorrepaal E, Toet S, van Logtestijn RS, Swart E, van de Weg MJ, Callaghan TV, Aerts R. 2009. Carbon respiration from subsurface peat accelerated by climate warming in the subarctic. *Nature* **460**(7255): 616-619.
- Edlund JG, Gordon G, Robinson P. 1998. A model mine shows its cracks. Unpublished report by *Pacific Environment*. [http://pacificenvironment.org/downloads/model\\_mine.pdf](http://pacificenvironment.org/downloads/model_mine.pdf)
- Forsstrom AM, Long EL, Zarling JP, Knutsson S. 2002. Thermosyphon cooling of Chena Hot Springs Road test section. *Proceedings of the 11th International Conference in Cold Regions Engineering*. ASCE, Anchorage, AK, 645–655.
- Garon-Labreque ME, Leveille-Bourret E, Higgins K, Sonnentag O. 2015. Additions to the boreal flora of the Northwest Territories with a preliminary vascular flora of Scotty Creek. *The Canadian Field Naturalist* **129**: 349–367.
- Goetz, P. 2010. Preserving Arctic archaeology in the 21st century: threats of climate change. University of Waterloo. Retrieved on March 11, 2020 from <https://uwspace.uwaterloo.ca/handle/10012/5660>

- Goodison BE, Walker AE. 1993. Use of snow cover derived from satellite microwave data as an indicator of climate change. *Annals of Glaciology* **17**: 137-142.
- Goodrich LE. 1982. The influence of snow cover on the ground thermal regime, *Canadian Geotechnical Journal* **19**(4), 421– 432.
- Gorham E. 1991. Northern Peatlands: Role in the Carbon Cycle and Probable Responses to Climatic Warming. *Ecological Applications* **1**(2): 182-195.
- Haag RW, Bliss LC. 1974. Functional Effects of Vegetation on the Radiant Energy Budget of Boreal Forest. *Canadian Geotechnical Journal* **11**(3): 374-379.
- Halsey LA, Vitt DH, Zoltai SC. 1995. Disequilibrium response of permafrost in boreal continental western Canada to climate change. *Climatic Change* **30**(1): 57–73.
- Hayley DW, Seto JTC, Grapel CK, Cathro DC, Valeriote MA. 2004. Performance of two rockfill dams with thermosyphons on permafrost foundations, Ekati Diamond Mine, NT. 57th Canadian Geotechnical Conference, Quebec City.
- Haynes KM, Connon RF, Quinton WL. 2018. Permafrost thaw induced drying of wetlands at Scotty Creek, NWT, Canada. *Environmental Research Letters* **13**(11).
- Hinzman LD *et al.* 2005. Evidence and implications of recent climate change in northern Alaska and other arctic regions. *Climate Change*. **73**(2): 251–98.
- Jafarov EE, Coon ET, Harp DR, Wilson CJ, Painter SL, Atchley AL, Romanovsky VE. 2018. Modeling the role of preferential snow accumulation in through talik development and hillslope groundwater flow in a transitional permafrost landscape. *Environmental Research Letters* **13**(10)
- Jarvis PG, James GB, Landsberg JJ. 1976. Coniferous forest. Case Studies, J. L. Monteith, Ed., *Vegetation and the Atmosphere*, Vol. 2, Academic Press, 171–240.
- Johannessen OM, Bengtsson L, Miles MW, Kuzmina SI, Semenov VA, Alekseev GV, Nagurnyi AP, Zakharov VF, Bobilev LP, Pettersson LH, Hasselmann K, Cattle HP. 2004. Arctic climate change: observed and modelled temperature and sea-ice variability. *Tellus A: Dynamic Meteorology and Oceanography* **56**(5): 559-560.
- Jones PD, Moberg A. 2003. Hemispheric and Large-Scale Surface Air Temperature Variations: An Extensive Revision and an Update to 2001. *Journal of Climate* **16**(2): 206-223.
- Jorgenson MT, Racine CH, Walters JC, Osterkamp TE. 2010. Permafrost degradation and ecological changes associated with a warming climate in central Alaska. *Climate Change* **48**(4): 551–579.
- Kaufmann MR. 1984. A canopy model (RM-CWU) for determining transpiration of subalpine forests. I. Model development. *Canadian Journal of Forest Research* **14**(2): 218-226.

- Kurylyk BL, Hayashi M, Quinton WL, McKenzie JM and Voss CI. 2016. Influence of vertical and lateral heat transfer on permafrost thaw, peatland landscape transition, and groundwater flow. *Water Resources Research* **52**(2): 1286-1305.
- Kwong JT, Gan TY. 1994. Northward migration of permafrost along the Mackenzie Highway and climatic warming. *Climatic Change* **26**(4): 399-419.
- Lara MJ, Genet H, McGuire AD, Euskirchen ES, Zhang Y, Brown DRN, Jorgenson MT, Romanovsky V, Breen A, Bolton WR. 2016. Thermokarst rates intensify due to climate change and forest fragmentation in an Alaskan boreal forest lowland. *Global Change Biology* **22**(2): 816–829.
- Lewkowicz A. 2008. Evaluation of miniature temperature-loggers to monitor snowpack evolution at mountain permafrost sites, northwestern Canada. *Permafrost and Periglacial Processes* **19**(3): 323-331.
- Liston GE, Hiemstra CA. 2011. The changing cryosphere: pan-arctic snow trends (1979–2009). *Journal of Climate* **24**(21): 5691–5712.
- Leuzinger S, Vogt R, Korner C. 2010. Tree surface temperature in an urban environment. *Agricultural and Forest Meteorology* **150**(1): 56–62
- Long EL, Zarling JP. 2004. Passive techniques for ground temperature control. *Thermal Analysis, Construction, and Monitoring Methods for Frozen Ground* (Ed. by Esch ED), 492. Reston, VA: American Society of Civil Engineers.
- MacFarlane AK. 2003. Vegetation response to seismic lines: edge effects and on-line succession. M.Sc thesis, Department of Renewable Resources, University of Alberta, Edmonton, Alberta.
- Marshall S, Oglesby RJ, Nolin AW. 2003. The predictability of winter snow cover over the western United States. *Journal of Climate* **16**(7): 1062-1073.
- Martin TA, Hinckley TM, Meinzer FC, Sprugel DG. 1999. Boundary layer conductance, leaf temperature and transpiration of *Abies amabilis* branches. *Tree Physiology* **19**(7): 435–443.
- McClymont AF, Hayashi M, Bentley LR, Christensen BS. 2013. Geophysical imaging and thermal modeling of subsurface morphology and thaw evolution of discontinuous permafrost. *Journal of Geophysical Research* **118**(3): 1826–1837.
- Mellander P, Lofvenius MO, Laudon H. 2007. Climate change impact on snow and soil temperature in boreal Scots pine stands. *Climatic Change* **85**(1): 179–193.

- Melnikov PI, Makarov VI, Plotnikov AA. 1981. The engineering-physical basis of temperature regime regulation of ground massifs in northern construction. *Engineering Geology* **18**(1-4): 165-174.
- Moore TR. 1987. Thermal regime of peatlands in subarctic eastern Canada. *Canadian Journal of Earth Sciences* **24**(7): 1352-1359.
- Olefeldt D, Goswami S, Grosse G, Hayes D, Hugelius G, Kuhry P, McGuire AD, Romanovsky VE, Sannel AB, Schuur EA, Turetsky MR. 2016. Circumpolar distribution and carbon storage of thermokarst landscapes. *Nature Communications* **7**: 1-11.
- Oberman NG, Mazhitova GG. 2001. Permafrost dynamics in the northeast of European Russia at the end of the 20<sup>th</sup> century. *Norwegian Journal of Geography* **55**(4): 241– 244.
- Osborne E, Richter-Menge J, Jeffries M. 2018. Arctic Report Card 2018, Executive Summary. Retrieved on March 11, 2020 from <http://www.arctic.noaa.gov/Report-Card>
- Petty GW. 2006. A First Course in Atmospheric Radiation. 2nd ed. Madison. Sundog Publishing.
- Pomeroy JW, Brun E. 2001. Physical properties of snow. Jones, H. G., Pomeroy, J. W., Walker, D. A., and Hoham, R. W. (eds.), *Snow Ecology*. Cambridge: Cambridge University Press, 45–126.
- Popov AP, Vaaz SL, Usachev AA. 2010. Review of the current conditions for the application of heat pipes (thermosyphons) to stabilize the temperature of soil bases under facilities in the far North. *Heat Pipe Science and Technology* **1**(1): 89–98.
- Prowse TD, Furgal C. 2009. Northern Canada in a changing climate: major findings and conclusions. *Ambio* **38**(5): 290–292.
- Quinton WL, Shirazi T, Carey SK, Pomeroy JW. 2005. Soil water storage and active layer development in a sub-alpine tundra hillslope, Southern Yukon Territory, Canada. *Permafrost and Periglacial Processes* **16**: 369–382.
- Quinton WL, Marsh P. 1999. A conceptual framework for runoff generation in a permafrost environment. *Hydrological Processes* **13**(16): 2563-2581.
- Quinton WL, Hayashi M, Pietroniro A. 2003. Connectivity and storage functions of channel fens and flat bogs in northern basins. *Hydrological Processes* **17**(18): 3665–3684.
- Quinton WL, Hayashi M and Chasmer LE. 2009. Peatland hydrology of discontinuous permafrost in the Northwest Territories: overview and synthesis. *Canadian Water Resources Journal* **34**(4): 311–328.
- Quinton W, Hayashi M, Chasmer L. 2011. Permafrost-thaw-induced land-cover change in the Canadian subarctic: implications for water resources. *Hydrological Processes* **25**(1): 152–158.

- Rahman MA, Saghir MZ. 2014. Thermosdiffusion or Soret Effect: Historical review. *International Journal of Heat and Mass Transfer* **73**: 693-705.
- Raynolds MK, Walker DA, Ambrosius KJ, Brown J, Everett KR, Kenevskiy M, Kofinas GP, Romanovsky VE, Shur Y, Webber PJ. 2014. Cumulative geocological effects of 62 years of infrastructure and climate change in ice-rich permafrost landscapes, Prudhoe Bay Oilfield, Alaska. *Global Change Biology* **20**(4): 1211-1224.
- Revel RD, Dougherty TD, Downing DJ. 1984. Forest Growth and Revegetation Along Seismic Lines. The University of Calgary Press, Calgary, Alberta.
- Richter-Menge J, Jeffries MO, Osborne E. 2018. The Arctic. “State of the Climate in 2017”. *Bulletin of American Meteorological Society* **99**(8): 143–173.
- Robinson SD, Moore TR. 2000. The influence of permafrost and fire upon carbon accumulation in high boreal peatlands, Northwest Territories, Canada. *Arctic, Antarctic and Alpine Research* **32**(2): 155–66.
- Romanovsky VE, Drozdov DS, Oberman NG, Malkova GV, Kholodov AL, Marchenko SS, Moskalenko NG, Sergeev DO, Ukraintseva NG, Abramov AA, Gilichinsky DA, Vasiliev AA. 2010. Thermal state of permafrost in Russia. *Permafrost and Periglacial Processes* **21**(2): 136-155.
- Schuur EA, Abbott B. 2011. Climate change: high risk of permafrost thaw. *Nature* **480**(7375): 31–33.
- Schuur EA *et al.* 2015. Climate change and the permafrost carbon feedback. *Nature* **520**(7546): 171–179.
- Semmens KA, Ramage JM. 2013. Recent changes in spring snowmelt timing in the Yukon River basin detected by passive microwave satellite data. *Cryosphere* **7**(3): 905-916.
- Simon T, Payette S. 2009. Recent permafrost degradation in bogs of the James Bay area, northern Quebec, Canada. *Permafrost and Periglacial Processes* **20**(4): 383-389
- Smith MW. 1975. Microclimatic influences on ground temperatures and permafrost distribution, Mackenzie Delta, Northwest Territories. *Canadian Journal of Earth Sciences* **12**(8): 1421-1438.
- Smith MW, Riseborough DW. 1983. Permafrost sensitivity to climatic change. *Proceedings, Fourth International Conference on Permafrost*, 17-22 July 1983, Fairbanks, AK. Washington, D.C.: National Academy Press. Vol. 1: 1178-1183.
- Smith TM, Reynolds RW. 2005. A Global Merged Land–Air–Sea Surface Temperature Reconstruction Based on Historical Observations (1880–1997). *Journal of Climate* **18**(12): 2021-2036.

- Spittlehouse DL, Adams RS, Winkler RD. 2004. Forest, edge and opening microclimate at Sicamous Creek. British Columbia Ministry of Forests Research Program Research Report 24: 55.
- Tarnocai C, Stolbovoy V. 2006. Northern peatlands: Their characteristics, development and sensitivity to climate change. In: Martini IP, Martinez Cortizas A, Chesworth W (Eds.), Peatlands: Evolution and Records of Environmental and Climate Changes. Amsterdam, Netherlands, Elsevier BV, Chapter 2: 17–51.
- Tarnocai C. 2006. The effect of climate change on carbon in Canadian peatlands. *Global Planetary Change* **53**(4): 222–232.
- Turunen J, Tomppo E, Tolonen K, Reinikainen A. 2002. Estimating carbon accumulation rates of undrained mires in Finland – application to boreal and subarctic regions. *The Holocene* **12**(1): 79-90.
- Turetsky MR, Wieder RK, Vitt DH, Evans RJ, Scott KD. 2007. The disappearance of relict permafrost in boreal north America: effects on peatland carbon storage and fluxes. *Global Change Biology* **13**(9): 1922–1934.
- Vose RS, Easterling DR, Gleason B. 2005. Maximum and minimum temperature trends for the globe: An update through 2004. *Geophysical Research Letters* **32**(23): L23822
- Waddington JM, Strack M, Greenwood MJ. 2010. Toward restoring the net carbon sink function of degraded peatlands: Short-term response in CO<sub>2</sub> exchange to ecosystem-scale restoration. *Journal of Geophysical Research: Biogeosciences* **115**(G1).
- Warren RK, Pappas C, Helbig M, Chasmer LE, Berg AA, Baltzer JL, Quinton WL, Sonnetag O. 2018. Minor contribution of overstory transpiration to landscape evapotranspiration in boreal permafrost peatlands. *Ecohydrology* **11**(5): e1975.
- Wen Z, Sheng Y, Ma W, Qi JL, Jichun W. 2005. Analysis on effect of permafrost protection by two-phase closed thermosyphon and insulation jointly in permafrost regions. *Cold Regions Science and Technology* **43**(3): 150–163.
- Whittington PN, Price JS. 2006. The effects of water table draw-down (as a surrogate for climate change) on the hydrology of a fen peatland, Canada. *Hydrological Processes* **20**(17): 3589-3600.
- Williams TJ, Quinton WL and Baltzer JL. 2013. Linear disturbances on discontinuous permafrost: implications for thaw-induced changes to land cover and drainage patterns. *Environmental Research Letters* **8**(2): p.025006.
- Xu J, Goering DJ. 2008. Experimental validation of passive permafrost cooling systems. *Cold Regions Science and Technology* **53**(3): 283–297.
- Zarling JP, Brayley WA. 1987. Thaw stabilization of roadway embankments constructed over permafrost. Fairbanks, AK: AK Department of Transportation and Public Facilities.

Zhang T, Armstrong RL. 2001. Soil freeze/thaw cycles over snow-free land detected by passive microwave remote sensing. *Geophysical Research Letters* **28**(5): 763-766.

Zhang T. 2005. Influence of the seasonal snow cover on the ground thermal regime: An overview. *Reviews of Geophysics* **43**(4).

Zhang F, Zhang H, Hagen SC, Ye M, Wang D, Gui D, Zeng C, Tian L, Liu J. 2015. Snow cover and runoff modelling in a high mountain catchment with scarce data: effects of temperature and precipitation parameters. *Hydrological Processes* **29**(1): 52-65.

Zoltai SC. 1993. Cyclic development of permafrost in the peatlands of Northwestern Alberta, Canada. *Arctic and Alpine Research* **25**(3): 240–246.